



The Roles of Resuspension, Diffusion and Biogeochemical Processes on Oxygen Dynamics Offshore of the Rhone River, France: A Numerical Modeling Study

5 Julia M. Moriarty¹, Courtney K. Harris¹, Christophe Rabouille², Katja Fennel³, Marjorie A. M. Friedrichs¹, Kehui Xu^{4,5}

¹Virginia Institute of Marine Science, the College of William & Mary, Hayes, Virginia, 23062 USA

²Laboratoire des Sciences du Climat et de l'Environnement, UMR CEA-CNRS-UVSQ and IPSL, Gif sur Yvette 91198, France

³Department of Oceanography, Dalhousie University, Halifax, Nova Scotia B3P 2A3, Canada

10 ⁴Department of Oceanography and Coastal Sciences, Louisiana State University, Baton Rouge, Louisiana 70803, USA

⁵Coastal Studies Institute, Louisiana State University, Baton Rouge, Louisiana 70803, USA

Correspondence to: Julia M. Moriarty (moriarty@vims.edu)

Abstract. Observations indicate that seabed resuspension of organic material and the associated entrainment of porewater
15 into the overlying water can alter biogeochemical fluxes in some environments, but measuring the role of sediment processes on oxygen and nutrient dynamics is challenging. A modeling approach offers a means of quantifying these fluxes for a range of conditions, but models have typically relied on simplifying assumptions regarding seabed-water column interactions. Thus, to evaluate the role of resuspension on biogeochemical dynamics, we developed a coupled hydrodynamic, sediment transport, and biogeochemical model (HydroBioSed) within the Regional Ocean Modeling System (ROMS). This coupled
20 model accounts for processes including the storage of particulate organic matter (POM) and dissolved nutrients within the seabed; entrainment of this material into the water column via resuspension and diffusion at the sediment-water interface; and biogeochemical reactions within the seabed. A one-dimensional version of HydroBioSed was then implemented for the Rhone Delta, France. To isolate the role of resuspension on biogeochemical dynamics, this model implementation was run for a two-month period that included three resuspension events; also, the supply of organic matter, oxygen and nutrients to
25 the water column was held constant in time. Consistent with time-series observations from the Rhone Delta, model results showed that resuspension increased the diffusive flux of oxygen into the seabed by increasing the vertical gradient of oxygen at the seabed-water interface. This enhanced supply of oxygen to the seabed allowed seabed oxygen consumption to increase, primarily through nitrification. Resuspension of POM into the water column, and the associated increase in remineralization, also increased oxygen consumption in the bottom boundary layer. During these resuspension events,
30 modeled rates of oxygen consumption increased by up to factors of ~2 and ~8 in the seabed and bottom boundary layer, respectively. When averaged over two months, the intermittent cycles of erosion and deposition led to a 20% increase of oxygen consumption in the seabed, as well as a larger increase of ~200% in the bottom boundary layer. These results imply that observations collected during quiescent periods, and biogeochemical models that neglect resuspension or use typical



parameterizations for resuspension, may underestimate net oxygen consumption at sites like the Rhone Subaqueous Delta. Local resuspension likely has the most pronounced effect on oxygen dynamics at study sites with a high oxygen concentration in the bottom boundary layer, only a thin seabed oxic layer, and abundant labile organic matter.

1 Introduction

5 Understanding and quantifying the role that physical processes play on coastal water quality remains a scientific and management concern. Management solutions to hypoxia, the occurrence of low oxygen concentrations, as well as other water quality issues, have focused on reducing riverine delivery of nutrients and sediments (Bricker et al., 2007). Yet temporal lags between these reductions and water quality improvements (Kemp et al., 2009), and increased cycling of nutrients within coastal systems (e.g. Testa and Kemp, 2012), indicate that temporary storage of nutrients in the seabed and
10 subsequent release to the water column via diffusion and/or resuspension can affect water quality in some coastal environments. Neglecting these processes impairs managers' ability to develop and evaluate strategies for improving coastal water quality (e.g. Artioli et al., 2008).

Resuspension-induced fluxes of sediment, particulate organic matter (POM), and dissolved chemical species between the
15 seabed and water column can significantly affect biogeochemistry in coastal waters, including oxygen dynamics (Glud, 2008). Entrainment of seabed organic matter and reduced chemical species into the water column can increase remineralization and oxidation rates, thereby decreasing oxygen concentrations in the bottom boundary layer (BBL) in some environments. For example, Abril et al. (1999) observed that oxygen concentrations were inversely correlated with tidal fluctuations of suspended particulate matter concentrations in the Gironde Estuary, France. Recently, Toussaint et al. (2014)
20 observed that resuspension may also increase oxygen consumption in the seabed by collecting high-resolution time-series of microelectrode oxygen profiles on the Rhone River Subaqueous Delta. This experiment revealed increases in diffusive fluxes of oxygen from the water column to the seabed during erosional events. Other observational studies have estimated resuspension-induced increases in oxygen consumption within the seabed and bottom boundary layer using measurements of turbulent oxygen fluxes (Berg and Huettle, 2008) and erodibility experiments (e.g., Sloth et al., 1996). Yet, it remains
25 difficult to distinguish and quantify the relative influences of different biogeochemical (e.g. remineralization, oxidation) and physical (e.g. diffusion, resuspension) processes on oxygen dynamics in both the seabed and bottom boundary layer.

Hydrodynamic-biogeochemical models often complement observational studies of water quality (e.g. Moll and Radach, 2003; Aikman et al., 2014), but these simulations usually neglect or simplify seabed-water column fluxes. Water quality
30 models often assume that organic matter and nutrients reaching the seabed are permanently buried, instantaneously remineralized, resuspended without remineralization, or a combination thereof (e.g. Cerco et al., 2013; Fennel et al., 2013; Feng et al., 2015; Bruce et al., 2014; Liu et al., 2015). Yet, numerical experiments showed that switching among relatively



simple parameterization methods for seabed-water column fluxes can alter the estimated area of low-oxygen regions by about -50% to +100% in the Gulf of Mexico (Fennel et al., 2013). This sensitivity of modeled oxygen concentrations to choice of parameterization, as well as the observations of temporally variable oxygen fluxes discussed above, motivate development of a process-based model for seabed-water column fluxes.

5

We therefore developed a modeling approach that accounts for physical and biogeochemical processes at the seabed-water interface, including resuspension of POM and porewater, and implemented it for the dynamic Rhone Delta. Previously, one-dimensional box models with a few vertical levels have been used to study the role of organic matter resuspension on oxygen (Wainright and Hopkinson, 1997) and contaminant levels (Chang and Sanford, 2005). Additionally, three-dimensional
10 circulation models have been coupled to biogeochemical models with a single seabed layer and implemented to investigate the role of POM resuspension on Baltic Sea carbon budgets (Almroth-Rosell et al., 2011) and Black Sea biogeochemistry (Capet et al., 2016). To the best of our knowledge, however, no existing models have sufficient vertical resolution to resolve changes in the vertical biogeochemical profiles that drive diffusive seabed-water column fluxes, or the ability to account for the entrainment of reduced chemical species into the water column.

15

This paper presents a model called *HydroBioSed* that can reproduce the mm-scale changes in seabed profiles of oxygen, nitrogen and carbon, as well as the resuspension-induced changes in seabed-water column fluxes observed on the Rhone River Subaqueous Delta, by coupling hydrodynamic, biogeochemical and sediment transport modules. This process-based
20 numerical model was implemented for the Rhone River Subaqueous Delta and used to evaluate how episodic storm resuspension and deposition affect millimeter-scale seabed biogeochemistry and overall oxygen consumption in a dynamic coastal environment. Specific research questions for this paper include: (1) How do resuspension and deposition affect the timing and magnitude of seabed and bottom boundary layer oxygen consumption? (2) What are the relative roles of resuspension, organic matter remineralization, and oxidation of reduced chemical species in controlling oxygen consumption in the seabed and bottom boundary layer? (3) How sensitive is oxygen consumption to resuspension frequency and
25 magnitude, sedimentation rate, organic matter lability and availability, rate of diffusion within the seabed, seabed nitrification rate, and other factors? (4) What characteristics of the study site lead to the dependence of oxygen dynamics on resuspension patterns?

1.1 Study Site

Located in the Gulf of Lions at the northwest end of the Mediterranean Sea, the Rhone River Subaqueous Delta in France is
30 an excellent study site for these research questions in part because of the available observational data (Fig. 1). The study site is co-located with the site from Toussaint et al. (2014) and is only a few km away from Site A in Pastor et al. (2011a); both sites are located in ~25 m water depth and are characterized by very similar biogeochemical characteristics (e.g. Rassmann et al., 2016), and so data from both locations were used for model input and evaluation. Importantly, data from Toussaint et al.



(2014) included a time-series of oxygen profiles with sub-millimeter scale resolution within the seabed and bottom cm of the water column. By resolving changes that occurred during resuspension events, Toussaint et al. (2014) showed that diffusion of oxygen into the seabed increased during resuspension events.

5 This study site experiences frequent seabed disturbance due to centimeters of resuspension superimposed on rapid fluvial deposition. Over timescales of decades, due to its proximity to the Rhone River (Fig. 1), this site has accumulated about 10 cm y^{-1} of sediment and 657 g $m^{-2} y^{-1}$ of carbon (Radakovitch et al., 1999; Pastor et al., 2011a), although sedimentation varies in response to seasonal and episodic changes in river discharge and wave energy (Pont, 1997; Miralles et al., 2006; Ulses et al., 2008; Cathalot et al., 2010). Deposition is punctuated by erosional events, and our study period, April-May 2012, 10 included 3 instances when waves induced 1-2 cm of resuspension (Toussaint et al., 2014). At this site, erosion and deposition are the main sources of seabed disturbance; little to no bioturbation has been observed (Pastor et al., 2011b).

The delivery of organic matter to the shelf drives oxygen consumption directly via aerobic remineralization, and indirectly, as reduced chemical species produced during remineralization are oxidized (Lansard et al., 2009). Organic material 15 comprises about 2-12% and <1-5% of water column and seabed particulate matter, respectively, and about four-fifths of it originates from a terrestrial source, with little marine influence at the study site (Bourgeois et al., 2011; Pastor et al., 2011a; Lorthiois et al., 2012; Cathalot et al., 2013). Yet, the material settling to the seabed at this site is relatively labile, and has been estimated to have remineralization rates of 11 - 33 y^{-1} in the water column (Pinazo et al., 1996) and 0.31 - 11 y^{-1} in the 20 seabed (Pastor et al., 2011a). Despite the large input of organic matter to the Gulf of Lions, oxygen concentrations remain near saturation and hypoxia has not been reported, likely because of energetic hydrodynamics (Rabouille et al., 2008). Seabed oxygen consumption decreases from about 20-30 mmol $O_2 m^{-2} d^{-1}$ in the prodelta to ~5 mmol $O_2 m^{-2} d^{-1}$ farther from the river mouth, consistent with a decrease in organic matter supply (Lansard et al., 2009). Yet, seabed fluxes of oxygen, carbon, and dissolved nutrients vary during resuspension events, complicating efforts to quantify the importance of different biogeochemical processes at this site (Lansard et al., 2009; Toussaint et al., 2014) and motivating this study.

25 2 Methods

This section describes HydroBioSed (Sect. 2.1), before explaining how it was implemented for the Rhone Delta and used to address the research questions (Sect. 2.2). Tables 1 and 2 list related symbols and vocabulary.

2.1 Model development

30 The fully coupled HydroBioSed numerical model was developed within the Regional Ocean Modeling System (ROMS), a community-based and well-utilized ocean modeling framework (Haidvogel et al., 2000, 2008; Shchepetkin, 2003; Shchepetkin and McWilliams, 2009). In addition to its core hydrodynamic components, ROMS includes widely-used



modules for sediment transport (CSTMS; Community Sediment Transport Modeling System; Warner et al., 2008), and water column biogeochemistry (e.g. Fennel et al., 2006; Fennel et al., 2013). We built on those previous studies by coupling the sediment transport and water column biogeochemistry components (Fig. 2), enabling the model to account for storage of POM and nutrients in the seabed, and subsequent resuspension and redistribution of the organic matter and nutrients. As part of the coupling, we also incorporated aggregation of detritus, seabed-water column diffusion, and a multi-layer seabed biogeochemical model based on Soetaert et al. (1996a, 1996b). Below, we briefly describe the sediment transport and water column biogeochemistry modules used, highlighting differences from standard ROMS implementations and the addition of the seabed biogeochemistry model.

2.1.1 Sediment transport module

Suspended sediment tracers in the ROMS-CSTMS module are transported via advection due to ocean currents; experience downward settling; may be deposited and resuspended from the multi-layer seabed model; and are subject to source and sink terms such as river discharge (Warner et al., 2008). Erosion from the seabed is parameterized such that resuspension may only occur when the modeled bed stress, τ_{bed} , exceeds the critical shear stress, $\tau_{crit,ised}$. The amount of sediment class *ised* that is eroded, E_{ised} , is estimated at each time step (parameters are defined in Table 1):

$$E_{ised} = M(1 - \Phi)f_{ised} \left(\frac{\tau_{bed} - \tau_{crit,ised}}{\tau_{crit,ised}} \right) \Delta t \quad (1)$$

Previous CSTMS applications accounted only for inert particulates; however, here we adapted the model to link sediment transport and biogeochemical processes. In HydroBioSed, POM from the water column biogeochemical module provides an additional source of particulates to the seabed (Sect. 2.1.3). Additionally, the seabed layering scheme was modified so that the seabed has sufficient resolution (<1 mm) near the seabed-water interface where vertical gradients in biogeochemical constituents such as dissolved oxygen can be high (Supplement S.2). Finally, while CSTMS already accounted for diffusion of sediment within the seabed (Sherwood et al., 2016), HydroBioSed also accounts for the diffusion of porewater and POM.

2.1.2 Water column biogeochemistry module

ROMS water column biogeochemistry modules have typically included variables for multiple nutrient, plankton and detrital classes and accounted for processes such as growth, grazing and remineralization (e.g. Fennel et al., 2006). Here, the ROMS biogeochemical model from Fennel et al. (2013) was modified so that HydroBioSed converts some of the water column detritus into faster-sinking aggregates (see Supplement S.1). These aggregates are partitioned into refractory and labile classes, and are remineralized as described in Fennel et al. (2006) for detritus. Aggregates are transported within the water column by the hydrodynamic module. Upon sinking to the bed, aggregates, as well as phytoplankton and detritus, are added to the pool of seabed organic matter within the seabed module, as described in the following section.



2.1.3 Seabed biogeochemistry module

A seabed biogeochemistry module (Soetaert et al., 1996a, 1996b) was added to ROMS to account for changes in oxygen, dissolved nitrogen, and POM due to remineralization, oxidation of reduced chemical species, and diffusion across the seabed-water interface. This model has performed well in many environments including areas near river deltas (Wijsman et al., 2002; Pastor et al., 2011a), on the continental shelf and slope (Soetaert et al., 1998; Epping et al., 2002), and in the deep ocean (Middelburg et al., 1996). To incorporate the Soetaert et al. (1996a, 1996b) model into HydroBioSed, we used the code developed by Wilson et al. (2013), and adapted it for the ROMS framework and the Rhone Delta.

This seabed biogeochemistry model specifically tracks degradable particulate organic carbon (POC), oxygen, nitrate, ammonium, and oxygen demand units (ODUs), defined as the moles of reduced chemical species that react with one molecule of O_2 when oxidized. Like Soetaert et al. (1996a, 1996b)'s early diagenetic model, HydroBioSed uses ODU to represent a combination of reduced chemical species that are produced during anoxic remineralization, including iron and manganese ions, sulfide, and methane. Modeled POC includes both labile and refractory (or semi-labile) classes. For a full model description, see Soetaert et al. (1996a, 1996b), but here we present the rate equations for oxic remineralization (Eq. 2), denitrification (Eq. 3), anoxic remineralization (Eq. 4), nitrification (Eq. 5) and oxidation of ODU (Eq. 6) to provide context for the Results and Discussion (see Table 1 for parameter definitions):

$$R_{aerobic} = \frac{POC}{dz} \times R_{POC} \left(\frac{O_2}{O_2 + k_{O_2}} \frac{1}{L_{tot}} \right) \quad (2)$$

$$R_{DNF} = \frac{POC}{dz} \times R_{POC} \left(\frac{l_{O_2}}{O_2 + l_{O_2}} \frac{NO_3}{NO_3 + k_{NO_3}} \frac{1}{L_{tot}} \right) \quad (3)$$

$$R_{anoxic} = \frac{POC}{dz} \times R_{POC} \left(\frac{l_{O_2, anoxic}}{O_2 + l_{O_2, anoxic}} \frac{l_{NO_3, anoxic}}{NO_3 + l_{NO_3, anoxic}} \frac{1}{L_{tot}} \right) \quad (4)$$

$$R_{nit} = \frac{NH_4}{dz} \times R_{nit, max} \left(\frac{O_2}{O_2 + k_{O_2, nit}} \right) \quad (5)$$

$$R_{oduox} = \frac{ODU}{dz} \times R_{odu, max} \left(\frac{O_2}{O_2 + k_{O_2, oduox}} \right) \quad (6)$$

L_{tot} , the non-dimensional sum of the limitation factors on remineralization processes, is:

$$L_{tot} = \left(\frac{O_2}{O_2 + k_{O_2}} \right) + \left(\frac{l_{O_2}}{O_2 + l_{O_2}} \frac{NO_3}{NO_3 + k_{NO_3}} \right) + \left(\frac{l_{O_2, anoxic}}{O_2 + l_{O_2, anoxic}} \frac{l_{NO_3, anoxic}}{NO_3 + l_{NO_3, anoxic}} \right) \quad (7)$$

Note that POC, O_2 , NO_3 , NH_4 , and ODU are stored in units of $mmol\ m^{-2}$ in the model, so they are divided by dz to provide a concentration and to be consistent with Soetaert et al. (1996a, 1996b).

Adaptations to the Soetaert et al. (1996a, 1996b) "early diagenesis" model that were made to merge it with the CSTMS and Fennel modules include neglecting seabed consolidation and temperature-induced changes to biogeochemical rates.



Specifically, HydroBioSed neglects changes in porosity with depth in the sediment bed because this study focused on the frequently resuspended surficial centimeter of the seabed and seabed-water column interactions. Also, we neglected the effect of temperature on remineralization rates and diffusion coefficients because temperature was held constant in time for this implementation of HydroBioSed (see Sect. 2.2).

5

Merging the Soetaert et al. (1996a, 1996b) seabed biogeochemical model with the sediment transport and water column biogeochemistry modules allows HydroBioSed to account for exchanges of biogeochemical tracers across the seabed-water interface due to erosion and deposition, as well as diffusion. In the CSTMS module, when bed shear stress exceeds the critical shear stress of the seabed, sediment may be entrained from the seabed into the water column (Eq. 1). In HydroBioSed, any POM or dissolved chemical species in the porewater within the resuspended seabed layer(s) is also entrained into the bottom water column layer. Similarly, during depositional periods, phytoplankton, detritus and aggregates settling to the seabed are incorporated into the surficial seabed layer. Upon deposition, the model adds phytoplankton, detritus and labile aggregates to the pool of labile seabed organic matter, whereas refractory aggregates are added to refractory organic matter. Porewater in newly deposited sediments is assumed to initially have concentrations of nutrients and oxygen equal to those in the overlying water column. In addition to resuspension, dissolved oxygen and nutrients may diffuse across the seabed-water interface as described in Soetaert et al. (1996a, 1996b) and Supplement S.2. Overall, HydroBioSed can represent POM in the seabed until it is resuspended, remineralized, or buried. Similarly, dissolved chemical species in the porewater may undergo biogeochemical transformations, diffuse into or out of the seabed, or be entrained into the water column during periods of erosion and deposition. Thus, unlike Soetaert et al. (1996a, 1996b) and other classical seabed biogeochemistry models (e.g. Boudreau, 1997; Soetaert et al., 2000; DiToro, 2001), HydroBioSed can quantify the effect of resuspension on biogeochemical dynamics (Fig. 2).

2.2 Model implementation and sensitivity tests

To evaluate the coupled model and explore the role of local resuspension on oxygen dynamics, we implemented a one-dimensional version of HydroBioSed for the Rhone Delta. This section describes the standard model run and sensitivity tests, and summarizes our methods for model evaluation and analysis. See Table 3 for a list of model input and parameters.

“Standard” Model Run: A one-dimensional (vertical) version of HydroBioSed was implemented for a 24-m deep site on the Rhone Subaqueous Delta (Fig. 1) for April-May 2012. This time period coincided with Toussaint et al. (2014)’s observational study and included three resuspension events as well as quiescent periods characterized by low bed stress. To implement a quasi one-dimensional model within the ROMS framework, a 5x6 model grid with spatially uniform forcing and periodic open boundary conditions was used. Vertical stratification in the model was maintained by strongly nudging temperature and salinity to climatological values; a pycnocline at 4 m above the seabed separated the colder saltier bottom boundary layer from the warmer fresher upper water column. Wave- and current-induced bed stresses were estimated using



the Sherwood, Signell and Warner (SSW) bottom boundary layer parameterization based on Madsen (1994) and described in Warner et al., (2008).

To isolate the effect of resuspension on seabed-water column fluxes, water column concentrations of oxygen, nitrogen, and ODU, as well as the supply of POM (excluding that from resuspension) were strongly nudged to temporally constant values. Hourly to daily oxygen observations from the bottom boundary layer (Toussaint et al., 2014) were used to constrain modeled concentrations in the water column. These observations indicated that oxygen concentrations 1 m above the bed varied between 216 - 269 mmol O₂ m⁻³, but that resuspension events did not appear to impact near-bed O₂ fluctuations. A constant value of 253 mmol O₂ m⁻³ was therefore used for water column O₂ concentrations (Pastor et al., 2011a). Values for water column nitrate, ammonium, and ODU concentrations were chosen based on Pastor et al. (2011a)'s Site A data because no observations were available from our study site (Fig. 1). Additionally, small detritus concentrations were strongly nudged to provide a constant supply of degradable POM to the water column equivalent to 657 gC m⁻² y⁻¹, based on Pastor et al. (2011a)'s estimate for organic sedimentation rate, S_{organic} . Nudging the small detritus did not affect the large detritus and aggregates that were resuspended from and deposited onto the seabed.

15

Model forcing and parameters were chosen based on a combination of observed values (wave height, bottom water oxygen concentrations), climatology (inorganic sedimentation rate, salinity, temperature), and values used in previously implemented models (fraction of labile material, nitrification rate, rates of diffusion within the seabed). See Table 3 for more details. A few parameters, i.e. critical shear stress for erosion and erosion rate parameter, were tuned to reproduce the 1-2 cm of observed erosion. For initialization, the model was run without resuspension until it reached steady state. The model used a 30 second time-step, saved its output in three-hour increments, and took ~6 hours to run on a single processor for a 2-month simulation.

Sensitivity Tests: In addition to the standard model run, seven sets of sensitivity tests examined the response of oxygen consumption to different parameters and processes (Table 4). These tests modified parameters related to resuspension and seabed processes, including the critical shear stress for erosion (τ_{crit}), erosion rate parameter (M), inorganic and organic sedimentation rates ($S_{\text{inorganic}}$ and S_{organic}), lability of aggregated organic matter (f_{lab}), rate of diffusion within the seabed (D_i), and nitrification rate in the seabed ($R_{\text{nit,max}}$). Additional tests modifying the ODU oxidation rate and the parameterization scheme for seabed-water column diffusion had a negligible effect on model results and so are not presented here.

30

Additionally, “no-resuspension” model runs were completed to evaluate the role of resuspension on biogeochemical dynamics; for each sensitivity test and the standard model run, a corresponding simulation was conducted that was identical to the original, except that resuspension was prevented by increasing the critical shear stress to $\tau_{\text{crit}} = 10$ Pa and decreasing



the erosion rate parameter to $M = 0 \text{ kg m}^{-2} \text{ s}^{-1}$. For conciseness, however, references to the “no-resuspension” model run refer to the no-resuspension version of the standard model, unless otherwise noted.

Model Analysis: We focused on seabed and bottom boundary layer oxygen consumption and on fluxes of oxygen at the seabed-water interface. The bottom boundary layer was defined as the region of the water column within 4 m of the seabed where suspended sediment concentrations were high during resuspension events. Concentrations and rates for analyses were saved in the model output, except for the magnitude of various biogeochemical sinks for oxygen within the bottom boundary layer, which were estimated based on the model equations and the concentrations of nutrients and POM saved in the model output. The fraction of oxygen consumption due to resuspension was calculated by dividing the difference between each sensitivity test and its no-resuspension model run by the value from the sensitivity test. Additionally, note that all POM estimates presented in this paper are for degradable organic matter. Although some studies add concentrations of inert POM to model estimates of degradable POM for comparison to observations, we plot only degradable POM for simplicity.

3 Results

This section evaluates the skill of the standard model run by comparing it to observations (Sect. 3.1), analyzes the effect of resuspension on oxygen dynamics (Sect. 3.2), and evaluates the results’ sensitivity to model parameters (Sect. 3.3).

3.1 Model evaluation

Comparison of the standard version of HydroBioSed to Toussaint et al. (2014)’s time-series of oxygen profiles showed that model results were consistent with measured concentrations, and changed during resuspension events in a manner similar to the observations (Fig. 3). During quiescent conditions when bed shear stress was low, modeled and observed oxygen concentrations decreased with depth into the seabed, falling from about $250 \text{ mmol O}_2 \text{ m}^{-3}$ in the bottom water column to $0 \text{ mmol O}_2 \text{ m}^{-3}$ within 1-2 mm below the seabed surface. Similarly, both the modeled and observed oxygen penetration depths decreased to about $<1 \text{ mm}$ in the seabed during times of erosion, before returning to equilibrium within hours of bed stresses returning to background values.

To quantify the changes in seabed oxygen profiles, the oxygen gradient near the seabed-water interface was calculated from both the observed and modeled profiles. Specifically, the slope of the oxygen profile was averaged over the oxygen penetration depth (OPD; symbols are given in Table 1):

$$\frac{dO_2}{dz_{OPD}} = \frac{O_{2,SWI} + O_{2,OPD}}{z_{SWI} + z_{OPD}} \quad (8)$$

Overall, dO_2/dz_{OPD} increased during erosional periods (Fig. 3; Table 5). During times when the seabed was not mobilized, dO_2/dz_{OPD} maintained a baseline of $\sim 100 \text{ mol O}_2 \text{ m}^{-4}$, in both the modeled results and the observed values. In contrast,



resuspension decreased the oxygen penetration depth, increasing dO_2/dz_{OPD} to about $500 \text{ mol O}_2 \text{ m}^{-4}$ (observed by Toussaint et al., 2014) and $900 \text{ mol O}_2 \text{ m}^{-4}$ (modeled).

Differences in the modeled and observed oxygen profiles derive at least partially from differences in estimating seabed elevation (i.e. resuspension and deposition). As a one-dimensional vertical model, HydroBioSed assumed uniform conditions in the horizontal, so that all resuspended material was re-deposited in the same location within a few days following an event. Yet, at the actual study site, it is likely that some material was carried out of the area and that deposition following the erosional periods was more gradual than estimated in the model (e.g. see the late April/early May event in Fig. 3c). Also, the model provided higher temporal resolution than possible with the sampling gear, and may capture peaks in dO_2/dz_{OPD} that are missed by the sampling frequency (Fig. 3d). Yet, in spite of these differences, HydroBioSed reproduced the general behavior of oxygen profiles as observed on the Rhone Subaqueous Delta (Fig. 3e,f,g). In contrast to previous models that could not account for resuspension-induced temporal variations (Pastor et al., 2011a), both observed and modeled dO_2/dz_{OPD} increased by factors of approximately 4-9 during erosional periods.

3.2 Response of oxygen dynamics to resuspension

Overall, the combined seabed-bottom boundary layer oxygen consumption increased from $\sim 40 \text{ mmol O}_2 \text{ m}^{-2} \text{ d}^{-1}$ to over $200 \text{ mmol O}_2 \text{ m}^{-2} \text{ d}^{-1}$ during resuspension events (Fig. 4b,c). Averaged over two months, resuspension roughly doubled the combined seabed-bottom boundary layer oxygen consumption to $>75 \text{ mmol O}_2 \text{ m}^{-2} \text{ d}^{-1}$. Although the seabed and bottom boundary layer contributed about equally to oxygen consumption during quiescent periods, the large increase in combined seabed-bottom boundary layer oxygen consumption during resuspension events was primarily driven by remineralization of POM in the bottom boundary layer (Table 6). For both the seabed and bottom boundary layer, resuspension added variability to oxygen dynamics, so that about one half of the total oxygen consumption occurred within the 30% of the two-month study period that included the resuspension events.

The cycles of erosion and deposition that affected biogeochemical cycles are illustrated by time-series of seabed profiles (Fig. 5). Before resuspension, the porewater in surface sediments was typically equilibrated with the overlying water column, with oxygen penetrating $\sim 1\text{-}2 \text{ mm}$ into the seabed. As energetic waves increased bed stresses, however, particulate matter from the seabed was eroded into overlying water, with typical erosion depths of $\sim 5\text{-}20 \text{ mm}$. This erosion of the surficial seabed exposed low-oxygen, high-ammonium, high-ODU porewater to the sediment-water interface. This exposure changed profiles, for example, by sharpening the oxygen gradient at the seabed-water interface and resuspending POM. As wave energy subsided and bed stresses decreased hours to a few days later, previously resuspended sediment and POM was re-deposited on the seabed. This re-deposited organic matter was particularly enriched in labile organic matter compared to the material that had remained on the seabed (see Supplement S.1). As new seabed layers formed from re-deposited sediments,



dissolved constituents from the overlying water were incorporated into the porewater of these new layer(s). This altered profiles by, for example, increasing the thickness of the oxic layer to a few mm during depositional periods.

The next two sections provide a more detailed and quantitative analysis of how these exchanges of porewater and particulate matter between the seabed and the overlying water increased oxygen consumption and affected related biogeochemical processes within the seabed (Sect. 3.2.1) and the bottom boundary layer (Sect. 3.2.2).

3.2.1 Seabed oxygen consumption

Resuspension directly altered the supply of oxygen to the seabed. In this environment, where oxygen penetration was limited to the top few millimeters of the seabed, resuspension events typically removed the entire seabed oxic layer; the oxygen that had been in the porewater was entrained into the water column. Similarly during deposition, incorporation of oxygen within the porewater of newly deposited sediment provided a source of oxygen to the seabed, accounting for up to a quarter of oxygen input to the seabed on a timescale of hours to days. Overall, this “pumping” of oxygen into and out of the seabed when sediments were deposited or eroded provided a small net source of oxygen to the seabed during a typical resuspension cycle; based on time-integrated fluxes of oxygen across the seabed-water interface for the two-month period (Fig. 6a), these exchanges accounted for 4% of the net oxygen supply to the seabed.

The remaining supply of oxygen (96%) was delivered to the seabed via diffusion across the seabed-water interface. Although these diffusive fluxes of oxygen were always directed into the seabed, erosion and deposition caused fluctuations in the rate of diffusion. During periods of resuspension, erosion of the oxic layer sharpened the oxygen gradient at the seabed-water interface, thus increasing diffusion of oxygen into the seabed by about 77% (Fig. 6a). In contrast, during periods of deposition, incorporation of oxygen-rich porewater into newly deposited surficial seabed layers reduced the oxygen gradient at the seabed-water interface, decreasing diffusion of oxygen into the seabed by about 71%. However, “erosional oxygen profiles” with thin oxygen penetration depths persisted longer and induced larger changes in the rate of diffusion, compared to “depositional oxygen profiles” with thick oxygen penetration depths. This imbalance occurred because the additional oxygen available in the seabed during periods of re-deposition (i.e., oxygen available due to the incorporation of oxic water into the porewater of newly-deposited sediments) was rapidly consumed, and so oxygen profiles returned to equilibrium within hours to ~1 day after a resuspension event. In contrast, during erosional periods, steep oxygen gradients and increased rates of diffusion into the seabed persisted for ~2-5 days (Fig. 6). Overall, averaged over two months, these resuspension-induced variations increased the rate of oxygen diffusion into the seabed by 12%.

In addition to impacting the supply of oxygen to the seabed, resuspension altered the magnitude of various biogeochemical oxygen sinks within the seabed (Table 6, Fig. 6b). For example, erosion of organic matter, and labile organic matter in particular, decreased rates of oxic remineralization in the seabed from about 5 to <1 mmol O₂ m⁻² d⁻¹ (e.g. compare the mid-



April quiescent period to the late April resuspension event). Simultaneously, entrainment of nitrate from the seabed into the water column, the augmented supply of oxygen to the seabed through erosion-enhanced diffusion, and the elevated concentration of ammonium in surficial seabed sediments all increased the rate of nitrification-related oxygen consumption from ~10-15 to ~30 mmol O₂ m⁻² d⁻¹. Together, these changes increased the fraction of oxygen consumed via nitrification from about 60-70% during quiescent periods to almost 95% during erosional periods. At the same time, the fraction of oxygen consumed via aerobic remineralization decreased from about 30-40% during quiescent periods to 4% during erosion. In contrast, following resuspension events, remineralization of redeposited organic matter, especially labile organic matter, briefly increased oxic remineralization rates. Also, low ammonium concentrations in newly deposited sediments limited nitrification during depositional periods. Together, these changes briefly altered the fraction of oxygen consumed via nitrification vs. remineralization to about 17% and 83%, respectively, during periods of re-deposition. Averaged over two months, however, resuspension-induced changes in the availability of oxygen, organic matter, and nutrients had little effect on the fraction of oxygen consumption due to nitrification (58%) and remineralization (41%).

3.2.2 Bottom boundary layer oxygen consumption

Resuspension primarily affected oxygen dynamics within the water column by entraining POM into the bottom boundary layer, which increased remineralization rates there (Table 6). Turbulence entrained this material as high as ~3-4 m above the seabed during resuspension events, with near-bed concentrations of POM reaching up to 5 x 10⁴ mmol C m⁻³ in the model. This material created an oxygen demand capable of consuming up to ~160 mmol O₂ m⁻² d⁻¹ during resuspension events.

In addition to entraining POM into the water column, resuspension increased fluxes of reduced chemical species from the seabed to the bottom boundary layer, further increasing oxygen consumption in the water column (Table 6). During quiescent periods, oxidation of ammonium (nitrification) and ODUs resulted in a background level of oxygen consumption of ~13 mmol O₂ m⁻² d⁻¹ in the bottom boundary layer. During erosion, the steepening of gradients increased the diffusive fluxes at the seabed-water interface from near zero to up to about 25 mmol m⁻² d⁻¹ of NH₄ and 3 mmol m⁻² d⁻¹ of ODU, increasing the supply of these reduced chemical species to the bottom boundary layer. Direct entrainment of ammonium and ODUs into the water column provided an additional ~5-10 mmol m⁻² d⁻¹ of NH₄ and <1 mmol m⁻² d⁻¹ of ODU. The increased supply of NH₄ and ODU increased bottom boundary layer oxidation rates to up to ~20 mmol O₂ m⁻² d⁻¹ during resuspension events. Comparing this oxygen demand with the estimates of remineralization-related demand calculated above, oxidation of ammonium and ODUs accounted for ~10% of oxygen consumption in the bottom boundary layer during resuspension events. The remaining ~90% percent came from the remineralization of organic matter.

3.3 Sensitivity tests

Like the standard model run, results from every sensitivity test showed that resuspension increased seabed and bottom boundary layer oxygen consumption during both individual resuspension events, and when estimates were averaged over



two months. Also, oxygen consumption in the bottom boundary layer was larger than that in the seabed for every sensitivity test by at least a factor of ~ 5 during resuspension events and ~ 2 when results were averaged over two months. However, altering various parameters did affect the model estimates of oxygen consumption in both the seabed and bottom boundary layer, as explored in Sect. 3.3.1 and 3.3.2, respectively. Analysis focuses on the two-month average of oxygen consumption rate and the maximum rate of oxygen consumption from erosional periods (Fig. 7a, 8a). For both of these quantities we also computed the fraction of oxygen consumption induced by resuspension (Fig. 7b, 8b).

3.3.1 Seabed oxygen consumption: Sensitivity tests

Over timescales ranging from hours to two months, seabed oxygen consumption was more sensitive to changes in the rate of diffusion within the seabed (D_b , Cases B1 and B2; Fig. 7a) than any other parameter considered in the sensitivity tests (Table 4). Halving and doubling the diffusion coefficients changed the seabed oxygen consumption by -28% and 39%, respectively, when integrated over the two-month model run, and by -22% and 24% during individual resuspension events. These changes occurred because faster diffusion rates within the seabed more quickly transported oxygen deeper into the seabed, reducing oxygen levels in surface sediments, and thereby increasing the diffusion of oxygen through the seabed-water interface. Increasing D_b thus increased the supply of oxygen to the seabed, allowing for more seabed oxygen consumption. In contrast, lower diffusion rates within the seabed slowed the supply of oxygen to the seabed, reducing seabed oxygen consumption.

Within the standard model run and most sensitivity tests, resuspension accounted for about 14% of the cumulative seabed oxygen consumption when integrated over two months. The role of resuspension, however, was especially sensitive to the partitioning and delivery of organic matter. Altering the partitioning of organic matter between labile and refractory classes changed the effect of resuspension on seabed oxygen consumption by up to 75% over two months (Cases L1 and L2; Fig. 7b). Specifically, decreasing (increasing) the fraction of organic matter that is labile, f_{lab} , by 30% decreased (increased) the resuspension-induced fraction of the seabed oxygen consumption to 4% (28%), compared to 14% in the standard model run. By affecting the availability of labile organic matter in the seabed, changing f_{lab} also altered the total seabed oxygen consumption (Fig. 7a).

3.3.2 Bottom boundary layer oxygen consumption: Sensitivity tests

Oxygen consumption in the bottom boundary layer averaged over two months was more sensitive to changes in the critical shear stress for erosion, τ_{crit} , than the other parameters (Fig. 8a; Cases T1 and T2). Halving and doubling the critical shear stress changed time-averaged bottom boundary layer oxygen consumption by 50% and -35%, respectively. During individual resuspension events, the effect of halving and doubling this parameter was more moderate and resulted in 7% and -20% changes, respectively. These changes in oxygen consumption occurred because halving and doubling the critical stress for erosion changed the frequency of resuspension, i.e. the amount of time that $\tau_{bed} > \tau_{crit}$, from 36% of the time in the standard model run to 53% and 15%, respectively. Thus, decreasing the critical shear stress prolonged resuspension events, which



caused more seabed organic matter and porewater to be entrained into the water column, increasing oxygen consumption in the bottom boundary layer. In contrast, a larger critical shear stress shortened resuspension events, decreasing oxygen consumption there.

- 5 Within the standard model run and most sensitivity tests, resuspension accounted for about 57% of bottom boundary layer oxygen consumption when averaged over two months (Fig. 8b). Similar to the above analysis, the extent to which resuspension affected oxygen consumption was especially sensitive to the critical shear stress (Cases T1, T2). Over the two-month model run, halving (doubling) the critical shear stress changed the fraction of bottom boundary layer oxygen consumption that occurred due to resuspension to 34% (71%).

10 4 Discussion

This discussion focuses on the importance of resuspension-induced changes in oxygen budgets in different environments (Sect. 4.1); compares our approach to other modeling techniques (Sect. 4.2); and suggests future research (Sect. 4.3).

4.1 Resuspension-induced increases in oxygen consumption

- 15 Resuspension-induced oxygen consumption that occurred during short-lived (hours to days) events increased model estimates of oxygen consumption integrated over longer timescales of weeks to months (Fig. 9). In other words, erosion and deposition did not just add variability to time-series of oxygen consumption; resuspension changed the oxygen budget of the Rhone Subaqueous Delta. This section discusses the environmental conditions that caused this effect and the extent to which we expect resuspension to increase oxygen consumption in other coastal systems (Sect. 4.1.1); and the importance of these changes relative to seasonal variability (Sect. 4.1.2).

20 4.1.1 Why does resuspension change oxygen consumption on the Rhone Delta?

- 25 Several characteristics of the Rhone Subaqueous Delta favor the importance of resuspension for estimates of oxygen consumption. First, frequent resuspension events, i.e. three events in two months (Fig. 3c), ensure that erosional seabed profiles and the entrainment of seabed organic matter into the water column occur often, increasing resuspension-induced oxygen consumption in both the seabed and bottom boundary layer. Second, oxygen concentrations near the seabed-water interface are relatively high, i.e. over 200 mmol O₂ m⁻³ (Fig. 3e,f,g), ensuring that oxygen is available to be consumed. Third, the seabed at this site on the Rhone Delta experiences little to no biological mixing (Pastor et al., 2011a). This encourages the formation of a relatively thin oxic layer that is easily resuspended, allowing erosional seabed profiles that increase seabed oxygen consumption to form frequently. Forth, organic matter and/or reduced chemical species concentrations are high in surficial sediments relative to the water column (e.g. Pastor et al., 2011a). This ensures that erosion provides a significant
30 supply of organic matter to the water column for remineralization and/or reduced chemical species for oxidation, increasing



oxygen consumption in the bottom boundary layer during resuspension events. Also, the large amount of labile organic matter and reduced chemical species in the seabed facilitates resuspension-induced seabed oxygen consumption by quickly consuming oxygen via remineralization or oxidation during resuspension events. The speed of oxygen consumption is important for the maintenance of erosional seabed profiles throughout the entire erosional period. Fifth, remineralization rates in the bottom boundary layer are fast compared to particle settling times, ensuring oxygen can be consumed in the bottom boundary layer before organic matter settles back to the seabed. The rates used in the model imply that ~3% of suspended POM is remineralized each day, and resuspension events often last for days on the Rhone Delta (Table 3, Fig. 4).

We expect that resuspension is also important for oxygen dynamics in other systems similar to the Rhone Subaqueous Delta. For seabed oxygen dynamics, the above requirements imply that the importance of resuspension increases in energetic, oxic, coastal areas with high organic matter input, but relatively little bioturbation, such as other river deltas (Aller, 1998; e.g. Amazon Delta, Brazil: Aller et al., 1996). For water column oxygen dynamics, the above criteria suggest that resuspension is most important in energetic, oxic, coastal areas with organic-rich, muddy seabeds, but relatively low background concentrations of organic matter in the water column. These characteristics may be found in regions with historically high nutrient loading and where organic matter has accumulated in the seabed (e.g. Gulf of Finland: Almroth et al., 2009). In sites that meet some, but not all of the above criteria, the effect of local resuspension on oxygen dynamics is likely reduced compared to the Rhone Subaqueous Delta.

4.1.2 How does resuspension-induced O₂ consumption compare to seasonal variability?

The model estimated that resuspension increased seabed and bottom boundary layer oxygen consumption by about 20% and 200%, respectively, when integrated over April-May 2012 (Fig. 7, 8, 9); however, seasonal variations in environmental conditions such as temperature may change the importance of resuspension for oxygen dynamics. The two-month model run presented here assumed a constant bottom water temperature of 15°C, but observed values vary from ~12–20 °C over the course of a year on the Rhone Delta (Millot, 1990; Fuchs and Pairaud, 2014; Rabouille, pers. comm.). A common method for estimating temperature-induced changes in biogeochemical processes is the “Q10 rule” (van’t Hoff, 1898), which implies that oxygen consumption increases by a factor of ~2.5 for each temperature increase of 10°C in coastal areas (e.g. Dedieu et al., 2007; Hetland and DiMarco, 2008; Murrell and Lehrter, 2011; Cardoso et al., 2014; Gahnström, 2016). Based on the 16±4 °C temperature range expected at this site over a year, this suggests that resuspension-induced changes in oxygen consumption are as important as the factor of two change estimated due to temperature-induced variability. Thus, although temperature effects have been widely studied, resuspension can cause similar variations in oxygen consumption.

Seasonal variations in resuspension frequency and magnitude may have a similarly large effect on oxygen consumption. During the winter when easterly storms are more frequent (Guillén et al., 2006; Palanques et al., 2006), resuspension-induced oxygen consumption could be more important than was estimated for the April-May period in this study. At the 32



m deep “Sète” site in the central coastal region of the Gulf of Lions, significant wave heights exceeding 2 m were observed an average of 3.5, 1 and 2 times per month in November-December 2003, January-February 2004, and March-April 2004, respectively (Ulses et al., 2008). Approximately doubling the resuspension frequency during the winter storm season could roughly double resuspension-induced oxygen consumption, counteracting reductions in wintertime oxygen consumption due to colder temperatures. Overall, accounting for the effect of erosional and depositional cycles on oxygen consumption may vary in importance throughout the year on the Rhone Subaqueous Delta, but it is likely more important during Fall compared to the time period in Spring that was analyzed for this study.

4.2 Modeling resuspension-induced changes in oxygen dynamics

HydroBioSed differs from other models by accounting for resuspension-induced changes in millimeter-scale biogeochemistry, a feature that was necessary to produce Toussaint et al. (2014)’s observed temporal variations in seabed oxygen consumption on the Rhone Subaqueous Delta. In comparison, other models neglect resuspension-induced changes in biogeochemical dynamics or assume that seabed oxygen consumption decreases during erosion (e.g. Cerco et al., 2013; Feng et al., 2015; Wainright and Hopkinson, 1997). Specifically, the parameterizations in these other models account for increases in remineralization in the bottom boundary layer due to resuspension of organic matter, but they assume that it is offset by decreased remineralization and associated oxygen consumption in the seabed, causing them to underestimate seabed oxygen consumption during resuspension events. Results from these model parameterizations therefore conflict with observations and HydroBioSed results for the Rhone Subaqueous Delta (Fig. 4; Toussaint et al., 2014) that show that seabed oxygen consumption *increases* during resuspension events because of the increased diffusion of oxygen into the seabed during erosional periods. Alternate parameterizations for seabed-water column fluxes that focus on diffusion of oxygen across the seabed water interface instead of, or in addition to, organic matter supply (e.g. Findlay and Watling, 1997; De Gaetano et al., 2008; Hetland and DiMarco, 2008; Murrell and Lehrter, 2011; Testa et al., 2014) may be more appropriate for the Rhone Delta and similar environments.

The remainder of this section explores what sediment processes were most critical for modeling the effect of resuspension on Rhone Delta oxygen dynamics. First, resuspension increased the importance of the bottom boundary layer relative to the seabed. During quiescent conditions, the bottom boundary layer and seabed each accounted for similar rates of oxygen consumption. However, when POM and porewater were entrained into the water column via resuspension, bottom boundary layer oxygen consumption increased by a factor of eight, while seabed oxygen consumption only doubled. This disproportionate increase of oxygen consumption within the bottom boundary layer affirmed the importance of observing and modeling oxygen dynamics within the bottom boundary layer during resuspension events. Also, only accounting for quiescent time periods would underestimate the role of the bottom boundary layer, which accounted for 75% of the total oxygen consumption over the two-month model run for the Rhone Delta site, but only accounted for about 50% when resuspension was neglected.



Diffusion of oxygen across the sediment-water interface dominated the supply of oxygen to the seabed in the model, regardless of the timescale or time period considered. The other transport mechanism, the “pumping” of oxygen into and out of the seabed when sediments were deposited or eroded, provided at most a third of the flux to the seabed (during
5 depositional time periods; Fig. 5). Also, “pumping” contributed much less to seabed oxygen supply over time, primarily because the entrainment of porewater from the seabed into the water column during erosional periods partially offset the depositional flux of oxygen (Fig. 5). Over the two-month model simulation, diffusion across the seabed-water interface accounted for 96% of the seabed oxygen supply, whereas “pumping” due to erosion and deposition accounted for only 4% of
10 seabed oxygen fluxes. Thus, for environments like the Rhone Delta, future observational and modeling efforts should include resuspension-induced changes to diffusive fluxes across the seabed water interface (Jørgensen and Revsbech, 1985).

4.3 Implications of model development & future work

This study focused on oxygen dynamics while holding the supply of organic matter and sediment, as well as water column concentrations of nutrients and oxygen, constant in time. Yet, many coastal environments experience daily, tidal, seasonal, or inter-annual variations in their supply. On the Rhone Delta, for example, flood events may deliver relatively refractory
15 organic matter to the site, lowering seabed oxygen consumption in spite of the large quantity of riverine organic matter deposited on the shelf (e.g. Cathalot et al., 2010). Investigating how these temporal variations affect the relative importance of resuspension for oxygen dynamics could be useful for further extrapolating our results to different environments.

Our analysis focused on oxygen, but resuspension also affected model estimates of nitrogen dynamics. For example, during
20 quiescent periods, nitrification roughly balanced production of ammonium from remineralization of organic matter in the seabed. However, during erosional periods, the exposure of ammonium-rich porewater to oxygen increased seabed nitrification, enhancing fluxes of nitrate out of the seabed, consistent with observations from other systems (e.g. Fanning et al., 1982; Sloth et al., 1996; Tengberg et al., 2003). Overall, resuspension increased nitrate fluxes out of the seabed by about a factor of 2 during resuspension, which led to about a 10% increase overall for the two-month model run.

25

HydroBioSed did not represent all processes that occur near the seabed-water column interface, and so future work could include accounting for turbulence-induced changes in diffusion, advective fluxes through the seabed, and porosity variations in the seabed. Within HydroBioSed, for example, the steepening of the oxygen gradient at the seabed-water interface occurred because of changes in oxygen concentrations within the seabed and bottom boundary layer (Fig. 3). HydroBioSed
30 did not account for the thinning of the viscous layer at the seabed-water interface in response to wave-induced turbulence, which would act to further increase the oxygen gradient during erosional time periods (Gundersen and Jørgensen, 1990; Chatelain and Guizien, 2010; Wang et al., 2013). Neglecting this implies our current model may estimates of oxygen diffusion into the seabed during resuspension events are conservative. Additionally, the model could be adapted for locations



where waves and currents drive flows of water through non-cohesive seabeds, stimulating biogeochemical reactions (Huettel et al., 2014), or to account for vertical gradients in seabed porosity (Soetaert et al., 1996a, 1996b).

Applying HydroBioSed for a three-dimensional system would facilitate its application to more scientific and water quality concerns. For example, transport of organic matter from regions near the Mississippi and Atchafalaya river mouths, shallow autotrophic waters, and wetlands to “Dead Zones” has been speculated to encourage the depletion of oxygen in bottom waters there (Bianchi et al., 2010). However, the importance of organic matter transport within a single season of hypoxia, and on inter-annual timescales, is difficult to quantify with observations and has been debated on the northern shelf of the Gulf of Mexico (Rowe and Chapman, 2002; Boesch, 2003; Turner et al., 2008; Forrest et al., 2012; Eldridge and Morse, 2008) and other locations (Kemp et al., 2009 and references therein). Modeling efforts that account for resuspension of organic matter, as well as oxygen and nutrients, can help quantify the extent to which organic matter supply, resuspension and transport affect biogeochemical dynamics in these dynamic coastal environments (e.g. Capet et al., 2016).

Finally, this research effort incorporated time-dependent reactions into the ROMS’ sediment transport module and could be adapted for other research applications for which both resuspension and time-dependent tracers are important. For example, the model has been adapted to account for short-lived radioisotopes (Birchler, 2014) and could be adapted to include: particle-reactive nutrients and contaminants (Wiberg and Harris, 2002; Chang and Sanford, 2005); other non-conservative “particulates” such as harmful algal blooms (HAB) cysts (Beaulieu et al., 2005; Giannakourou et al., 2005; Butman et al., 2014; Kidwell, 2015) or fecal pellets (Gardner et al., 1985; Walsh et al., 1988); and temporal variability in organic matter lability, oxygen exposure time and carbon budgets (Aller, 1998; Hartnett et al., 1998; Burdige, 2007).

5 Summary and conclusions

A model called HydroBioSed was developed that couples hydrodynamics, sediment transport, and both water column and seabed biogeochemistry. A one-dimensional (vertical) version of the model was then implemented for the Rhone River Subaqueous Delta. This work expanded on the commonly used ROMS framework by accounting for non-conservative tracers; the resuspension of organic matter and entrainment of porewater into the water column; diffusion of dissolved tracers across the seabed-water interface; and feedbacks between resuspension and diffusion across the seabed-water interface. Including these processes created a new model capable of reproducing observed changes in seabed profiles that occurred during resuspension events, as observed by Toussaint et al. (2014) on the Rhone River sub-aqueous Delta.

Resuspension increased model estimates of seabed and bottom boundary oxygen consumption, over the range of timescales considered (hours to two months). In the seabed, resuspension increased the supply of oxygen by exposing anoxic sediment to oxygen-rich bottom waters during periods of erosion, which increased diffusion of oxygen across the seabed-water



interface. In the water column, resuspension entrained seabed organic matter and reduced chemical species from the porewater into the bottom boundary layer, increasing oxygen consumption there. Overall, resuspension increased peak oxygen consumption rates more in the bottom boundary layer (factor of eight) than in the seabed (factor of 2). When averaged over a two-month period that included intermittent periods of erosion and deposition, accounting for resuspension
5 increased oxygen consumption by 20% in the seabed and 200% in the bottom boundary layer. Overall, the combined seabed and bottom boundary layer oxygen consumption increased by a factor of about five during wave resuspension events and roughly doubled the two-month average.

These results imply that observations collected during quiescent periods, and models based on steady-state assumptions, may
10 underestimate net oxygen consumption. This finding is consistent with results from laboratory erodibility experiments (e.g. Sloth et al., 1996), observations using eddy correlation techniques (Berg and Huettle, 2008), and microelectrode profiles (Toussaint et al., 2014). While all of these studies showed increased oxygen consumption during resuspension events, they each had limitations; i.e., erodibility experiments are limited to low levels of erosion and timescales of hours, eddy-correlation methods can only be used for time periods without abrupt shifts in hydrodynamic and oxygen conditions (Lorrai
15 et al., 2010), and microelectrodes can only be deployed in soft muddy seabeds. Thus, models like HydroBioSed that resolve both biogeochemical processes and resuspension may help observational studies quantify oxygen dynamics over longer time periods, during storms, and in a variety of environments.

Certain characteristics of the Rhone Subaqueous Delta study site, including its oxic bottom boundary layer, shallow oxygen
20 penetration into the seabed compared to the thickness of eroded layers, fast rates of oxygen consumption, and the large supply of labile organic matter, enhance the effect of resuspension on oxygen dynamics. Together, these characteristics ensure that: oxygen is available to be supplied to the seabed during resuspension; erosion exposes anoxic regions of the seabed to oxic regions of the water column; oxygen consumption in the seabed is dependent on the supply of oxygen, as opposed to the rate of consumption; oxygen consumption in the bottom boundary layer is limited by the supply of organic
25 matter and reduced chemical species, as opposed to oxygen availability; and resuspended material is rich in organic matter and reduced chemical species that increases oxygen demand in the water column. The dependence of oxygen dynamics on those environmental conditions caused modeled estimates of oxygen consumption to be particularly sensitive to rates of diffusion within the seabed, nitrification rate, and the supply and lability of organic carbon. In addition, more frequent resuspension increased the importance of resuspension on oxygen dynamics. Our results imply that local resuspension may
30 affect oxygen dynamics in other environments with similar characteristics to those listed above.



Competing Interests

Katja Fennel is a member of the editorial board of the journal.

Acknowledgements

Observations and model code from previous publications were graciously provided by F. Toussaint (Laboratoire des
5 Sciences du Climat et de l'Environnement) and R. Wilson (formerly Dalhousie University). Feedback from E. Canuel and C.
Friedrichs (Virginia Institute of Marine Science; VIMS) has also improved this paper. A. Miller and D. Weiss (VIMS)
provided computational support. Funding was provided by the U.S. National Oceanic and Atmospheric Administration
Center for Sponsored Coastal Ocean Research (NA09NOS4780229, NA09NOS4780231, NGOMEX contribution
<*TBD*>) (Moriarty, Harris, Fennel, Xu), VIMS student fellowships (Moriarty), and MISTRALS/MERMEX-River and
10 ANR-11-RSNR-0002/ AMORAD (Rabouille). This is contribution <*TBD*> of the Virginia Institute of Marine Science.

References

- Abril, G., Etcheber, H., Le Hir, P., Bassoullet, P., Boutier, B., Frankignoulle, M.: Oxidic/anoxic oscillations and organic
carbon mineralization in an estuarine maximum turbidity zone (the Gironde, France), *Limnol. Oceanogr.*, 44, 1304–
1315. doi:10.4319/lo.1999.44.5.1304, 1999.
- 15 Aikman, F., Brady, D.C., Brush, M.J., Burke, P., Cerco, C.F., Fitzpatrick, J.J., Kemp, W.M.: Modeling approaches for
scenario forecasts of Gulf of Mexico hypoxia, in: Kidwell, D., Lewitus, A., Turner, E. (Eds.), White Paper from the
Hypoxic Zone Modeling Technical Review Meeting, Mississippi State University Science and Technology Center,
NASA's Stennis Space Center, Mississippi, pp. 1–46, 2014.
- Aller, R.C.: Mobile deltaic and continental shelf muds as suboxic, fluidized bed reactors, *Mar. Chem.*, 61, 143–155, 1998.
- 20 Aller, R.C.: Bioturbation and remineralization of sedimentary organic matter: effects of redox oscillation, *Chem. Geol.*, 114,
331–345. doi:10.1016/0009-2541(94)90062-0, 1994.
- Aller, R.C., Blair, N.E., Xia, Q., Rude, P.D.: Remineralization rates, recycling, and storage of carbon in Amazon shelf
sediments, *Cont. Shelf Res.*, 16, 753–786, doi:10.1016/0278-4343(95)00046-1, 1996.
- Almroth-Rosell, E., Eilola, K., Hordoir, R., Meier, H.E.M., Hall, P.O.J.: Transport of fresh and resuspended particulate
25 organic material in the Baltic Sea - a model study, *J. Mar. Syst.*, 87, 1–12, doi:10.1016/j.jmarsys.2011.02.005, 2011.
- Almroth, E., Tengberg, A., Andersson, J.H., Pakhomova, S., Hall, P.O.J.: Effects of resuspension on benthic fluxes of
oxygen, nutrients, dissolved inorganic carbon, iron and manganese in the Gulf of Finland, Baltic Sea, *Cont. Shelf Res.*,
29, 807–818. doi:10.1016/j.csr.2008.12.011, 2009.



- Artioli, Y., Friedrich, J., Gilbert, A.J., McQuatters-Gollop, A., Mee, L.D., Vermaat, J.E., Wulff, F., Humborg, C., Palmeri, L., Pollehne, F.: Nutrient budgets for European seas: A measure of the effectiveness of nutrient reduction policies, *Mar. Pollut. Bull.*, 56, 1609–1617, doi:10.1016/j.marpolbul.2008.05.027, 2008.
- Beaulieu, S.E., Sengco, M.R., Anderson, D.M. Using clay to control harmful algal blooms: deposition and resuspension of clay/algal flocs, *Harmful Algae*, 4, 123–138, doi:10.1016/j.hal.2003.12.008, 2005.
- Berg, P., Huettle, M.: Integrated benthic exchange dynamics, *Oceanography*, 21, 164–167, 2008.
- Bianchi, T.S., DiMarco, S.F., Cowan, J.H., Hetland, R.D., Chapman, P., Day, J.W., Allison, M. A.: The science of hypoxia in the Northern Gulf of Mexico: A review, *Sci. Total Environ.*, 408, 1471–84. doi:10.1016/j.scitotenv.2009.11.047, 2010.
- Birchler, J.J.: Sediment deposition and reworking: A modeling study using isotopically tagged sediment classes, Virginia Institute of Marine Science, the College of William & Mary, 2014.
- Boesch, D.F.: Continental shelf hypoxia: Some compelling answers: Comments on “Continental shelf hypoxia: Some nagging questions,” *Gulf Mex. Sci.*, 21, 143–145, 2003.
- Boudreau, B.P.: Diagenetic models and their implementation, Springer-Verlag, Berlin, Germany, 1997.
- Bourgeois, S., Pruski, A.M., Sun, M.-Y., Buscail, R., Lantoin, F., Vétion, G., Riviere, B., Charles, F.: Distribution and lability of land-derived organic matter in the surface sediments of the Rhone prodelta and the adjacent shelf (Mediterranean sea, France): A multi proxy study, *Biogeosciences Discuss.*, 8, 3353–3402, doi:10.5194/bg-8-3353-2011, 2011.
- Bricker, S.B., Longstaff, B., Dennison, W., Jones, A., Boicourt, K., Wicks, C., Woerner, J.: Effects of nutrient enrichment in the nation’s estuaries: A decade of change, *Harmful Algae*, doi:10.1016/j.hal.2008.08.028, 2007.
- Bruce, L.C., Cook, P.L.M., Teakle, I., Hipsey, M.R.: Hydrodynamic controls on oxygen dynamics in a riverine salt wedge estuary, the Yarra River estuary, Australia, *Hydrol. Earth Syst. Sci.*, 18, 1397–1411. doi:10.5194/hess-18-1397-2014, 2014.
- Burdige, D.J.: Preservation of organic matter in marine sediments: Controls, mechanisms, and an imbalance in sediment organic carbon budgets?, *Chem. Rev.*, 107, 467–485, doi:10.1021/cr050347q, 2007.
- Butman, B., Aretxabaleta, A.L., Dickhudt, P.J., Dalyander, P.S., Sherwood, C.R., Anderson, D.M., Keafer, B. A., Signell, R.P. Investigating the importance of sediment resuspension in Alexandrium fundyense cyst population dynamics in the Gulf of Maine, *Deep. Res. Part II Top. Stud. Oceanogr.*, 103, 79–95, doi:10.1016/j.dsr2.2013.10.011, 2014.
- Capet, A., Meysman, F.J.R., Akoumianaki, I., Soetaert, K., Grégoire, M.: Integrating sediment biogeochemistry into 3D oceanic models: A study of benthic-pelagic coupling in the Black Sea, *Ocean Model.*, 101, 83–100, doi:10.1016/j.ocemod.2016.03.006, 2016.
- Cardoso, S.J., Enrich-Prast, A., Pace, M.L., Rol, F.: Do models of organic carbon mineralization extrapolate to warmer tropical sediments?, *Limnol. Oceanogr.*, 59, 48–54, doi:10.4319/lo.2014.59.1.0048, 2014.



- Cathalot, C., Rabouille, C., Pastor, L., Deflandre, B., Viollier, E., Buscail, R., Gremare, A., Treignier, C., Pruski, A.: Temporal variability of carbon recycling in coastal sediments influenced by rivers: assessing the impact of flood inputs in the Rhone River prodelta, *Biogeosciences*, 7, 1187–1205, 2010.
- Cathalot, C., Rabouille, C., Tisnérat-Laborde, N., Toussaint, F., Kerhervé, P., Buscail, R., Loftis, K., Sun, M.-Y.Y., Tronczynski, J., Azoury, S., Lansard, B., Treignier, C., Pastor, L., Tesi, T.: The fate of river organic carbon in coastal areas: A study in the Rhône River delta using multiple isotopic ($\delta^{13}\text{C}$, $\Delta^{14}\text{C}$) and organic tracers, *Geochim. Cosmochim. Acta*, 118, 33–55, doi:10.1016/j.gca.2013.05.001, 2013.
- Cerco, C.F., Kim, S.-C.C., Noel, M.R.: Management modeling of suspended solids in the Chesapeake Bay, USA, *Estuar. Coast. Shelf Sci.*, 116, 87–98, doi:10.1016/j.ecss.2012.07.009, 2013.
- Chang, M.-L., Sanford, L.P.: Modeling the effects of tidal resuspension and deposition on early diagenesis of contaminants, *Aquat. Ecosyst. Heal.*, 8, 41–51, 2005.
- Chatelain, M., Guizien, K.: Modelling coupled turbulence - dissolved oxygen dynamics near the sediment-water interface under wind waves and sea swell, *Water Res.*, 44, 1361–72, doi:10.1016/j.watres.2009.11.010, 2010.
- Cruzado, A., Velasquez, Z.R.: Nutrients and phytoplankton in the Gulf of Lions, northwestern Mediterranean, *Cont. Shelf Res.* 10, 931–942, doi:10.1016/0278-4343(90)90068-W, 1990.
- Curran, K.J., Hill, P.S., Milligan, T.G., Mikkelsen, O. A., Law, B. A., Durrieu de Madron, X., Bourrin, F.: Settling velocity, effective density, and mass composition of suspended sediment in a coastal bottom boundary layer, Gulf of Lions, France, *Cont. Shelf Res.*, 27, 1408–1421, doi:10.1016/j.csr.2007.01.014, 2007.
- De Gaetano, P., Doglioli, A.M., Magaldi, M.G., Vassallo, P., Fabiano, M.: FOAM, a new simple benthic degradative module for the LAMP3D model: an application to a Mediterranean fish farm, *Aquac. Res.*, 39, 1229–1242, doi:10.1111/j.1365-2109.2008.01990.x, 2008.
- Dedieu, K., Rabouille, C., Thouzeau, G., Jean, F., Chauvaud, L., Clavier, J., Mesnage, V., Ogier, S. Benthic O₂ distribution and dynamics in a Mediterranean lagoon (Thau, France): An in situ microelectrode study, *Estuar. Coast. Shelf Sci.*, 72, 393–405, doi:10.1016/j.ecss.2006.11.010, 2007.
- DiToro, D.: *Sediment Flux Modeling*, Wiley-Interscience, 2001.
- Eldridge, P.M., Morse, J.W.: Origins and temporal scales of hypoxia on the Louisiana shelf: Importance of benthic and sub-pycnocline water metabolism, *Mar. Chem.*, 108, 159–171, doi:10.1016/j.marchem.2007.11.009, 2008.
- Epping, E., Zee, C. Van Der, Soetaert, K., Helder, W., van der Zee, C., Soetaert, K., Helder, W.: On the oxidation and burial of organic carbon in sediments of the Iberian margin and Nazare Canyon (NE Atlantic), *Prog. Oceanogr.*, 52, 399–431, 2002.
- Fanning, K.A., Carder, K.L., Betzer, P.R.: Sediment resuspension by coastal waters: A potential mechanism for nutrient recycling on the ocean's margins, *Deep Sea Res.*, 29, 953–965, 1982.



- Feng, Y., Friedrichs, M.A.M., Wilkin, J., Tian, H., Yang, Q., Hofmann, E.E., Wiggert, J.D., Hood, R.R.: Chesapeake Bay nitrogen fluxes derived from a land-estuarine ocean biogeochemical modeling system: Model description, evaluation and nitrogen budgets, *J. Geophys. Res. Biogeosciences*, 120, 1666–1695, doi:10.1002/2015JG002931, 2015.
- Fennel, K., Hu, J., Laurent, A., Marta-Almeida, M., Hetland, R.: Sensitivity of hypoxia predictions for the northern Gulf of Mexico to sediment oxygen consumption and model nesting, *J. Geophys. Res. Ocean.*, 118, 990–1002, doi:10.1002/jgrc.20077, 2013.
- Fennel, K., Wilkin, J., Levin, J., Moisan, J., O'Reilly, J., Haidvogel, D.: Nitrogen cycling in the Middle Atlantic Bight: Results from a three-dimensional model and implications for the North Atlantic nitrogen budget, *Global Biogeochem. Cycles*, 20, doi:10.1029/2005GB002456, 2006.
- 10 Ferré, B., Guizien, K., Durrieu De Madron, X., Palanques, A., Guillén, J., Grémare, A.: Fine-grained sediment dynamics during a strong storm event in the inner-shelf of the Gulf of Lion (NW Mediterranean), *Cont. Shelf Res.*, 25, 2410–2427, doi:10.1016/j.csr.2005.08.017, 2005.
- Findlay, R.H., Watling, L.: Prediction of benthic impact for salmon net-pens based on the balance of benthic oxygen supply and demand, *Mar. Ecol. Prog. Ser.*, 155, 147–157, 1997.
- 15 Forrest, D.R., Hetland, R.D., DiMarco, S.F.: Corrigendum: Multivariable statistical regression models of the areal extent of hypoxia over the Texas–Louisiana continental shelf, *Environ. Res. Lett.*, 7, 19501, doi:10.1088/1748-9326/7/1/019501, 2012.
- Fuchs, R., Pairaud, I.: Study of high frequency measurements from the MesuRho mooring, *Ifremer*, 1–39, 2014.
- Gahnström, G.: Sediment oxygen uptake in the acidified Lake Gardsjon, Sweden. *Ecol. Appl.*, 276–286, 2016.
- 20 Gardner, W.D., Southard, J.B., Hollister, C.D.: Sedimentation, resuspension and chemistry of particles in the Northwest Atlantic, *Mar. Geol.*, 65, 199–242, 1985.
- Giannakourou, A., Orlova, T.Y., Assimakopoulou, G., Pagou, K.: Dinoflagellate cysts in recent marine sediments from Thermaikos Gulf, Greece: Effects of resuspension events on vertical cyst distribution, *Cont. Shelf Res.*, 25, 2585–2596, doi:10.1016/j.csr.2005.08.003, 2005.
- 25 Glud, R.N.: Oxygen dynamics of marine sediments, *Mar. Biol. Res.*, 4, 243–289, doi:10.1080/17451000801888726, 2008.
- Guillén, J., Bourrin, F., Palanques, A., Durrieu de Madron, X., Puig, P., Buscail, R.: Sediment dynamics during wet and dry storm events on the Têt inner shelf (SW Gulf of Lions), *Mar. Geol.*, 234, 129–142, doi:10.1016/j.margeo.2006.09.018, 2006.
- Gundersen, J.K., Jorgensen, B.B.: Microstructure of diffusive boundary layers and the oxygen uptake of the sea floor, *Nature*, 345, 604–607, doi:10.1038/345604a0, 1990.
- 30 Haidvogel, D.B., Arango, H., Budgell, W.P., Cornuelle, B.D., Curchitser, E., Di Lorenzo, E., Fennel, K., Geyer, W.R., Hermann, A.J., Lanerolle, L., Levin, J., McWilliams, J.C., Miller, A.J., Moore, A.M., Powell, T.M., Shchepetkin, A.F., Sherwood, C.R., Signell, R.P., Warner, J.C., Wilkin, J.: Ocean forecasting in terrain-following coordinates: Formulation



- and skill assessment of the Regional Ocean Modeling System, *J. Comput. Phys.*, 227, 3595–3624, doi:10.1016/j.jcp.2007.06.016, 2008.
- Haidvogel, D.B., Arango, H.G., Hedstrom, K., Beckmann, A., Malanotte-Rizzoli, P., Shchepetkin, A.F. Model evaluation experiments in the North Atlantic Basin: simulations in nonlinear terrain-following coordinates, *Dyn. Atmos. Ocean*, 32, 239–281, doi:10.1016/S0377-0265(00)00049-X, 2000.
- Harris, C.K., Wiberg, P.L.: Approaches to quantifying long-term continental shelf sediment transport with an example from the Northern California STRESS mid-shelf site, *Cont. Shelf Res.*, 17, 1–30, doi:10.1016/S0278-4343(97)00017-4, 1997.
- Hartnett, H.E., Keil, R.G., Hedges, J.I., Devol, A.H.: Influence of oxygen exposure time on organic carbon preservation in continental margin sediments, *Nature*, 391, 572–575, doi:10.1038/35351, 1998.
- 10 Hetland, R.D., DiMarco, S.F.: How does the character of oxygen demand control the structure of hypoxia on the Texas–Louisiana continental shelf?, *J. Mar. Syst.*, 70, 49–62, doi:10.1016/j.jmarsys.2007.03.002, 2008.
- Huettel, M., Berg, P., Kostka, J.E.: Benthic exchange and biogeochemical cycling in permeable sediments, *Ann. Rev. Mar. Sci.*, 6, 23–51, doi:10.1146/annurev-marine-051413-012706, 2014.
- Jolliff, J.K., Kindle, J.C., Shulman, I., Penta, B., Friedrichs, M.A.M., Helber, R., Arnone, R.A.: Summary diagrams for coupled hydrodynamic-ecosystem model skill assessment, *J. Mar. Syst.*, 76, 64–82, doi:10.1016/j.jmarsys.2008.05.014, 2009.
- Jørgensen, B.B., Revsbech, N.P.: Diffusive boundary layers and the oxygen uptake of sediments and detritus, *Limnol. Oceanogr.*, 30, 111–122, doi:10.4319/lo.1985.30.1.0111, 1985.
- Kemp, W.M., Testa, J.M., Conley, D.J., Gilbert, D., Hagy, J.D.: Temporal responses of coastal hypoxia to nutrient loading and physical controls, *Biogeosciences*, 6, 2985–3008, doi:10.5194/bg-6-2985-2009, 2009.
- 20 Kidwell, D.: Mitigation of harmful algal blooms: The way forward, *PICES Press*, 23, 22–24, 2015.
- Lampitt, R.S., Raine, R.C.T., Billett, D.S.M., Rice, A.L.: Material supply to the European continental slope: A budget based on benthic oxygen demand and organic supply, *Deep. Res. Part I*, 42, 1865–1880, 1995.
- Lansard, B., Rabouille, C., Denis, L., Grenz, C.: Benthic remineralization at the land–ocean interface: A case study of the Rhône River (NW Mediterranean Sea), *Estuar. Coast. Shelf Sci.*, 81, 544–554, doi:10.1016/j.ecss.2008.11.025, 2009.
- Law, B. a., Hill, P.S., Milligan, T.G., Curran, K.J., Wiberg, P.L., Wheatcroft, R. A.: Size sorting of fine-grained sediments during erosion: Results from the western Gulf of Lions, *Cont. Shelf Res.*, 28, 1935–1946, doi:10.1016/j.csr.2007.11.006, 2008.
- Liu, K.K., Yan, W., Lee, H.J., Chao, S.Y., Gong, G.C., Yeh, T.Y.: Impacts of increasing dissolved inorganic nitrogen discharged from Changjiang on primary production and seafloor oxygen demand in the East China Sea from 1970 to 2002, *J. Mar. Syst.*, 141, 200–217, doi:10.1016/j.jmarsys.2014.07.022, 2015.
- 30 Lorrai, C., McGinnis, D.F., Berg, P., Brand, A., Wüest, A.: Application of Oxygen Eddy Correlation in Aquatic Systems, *J. Atmos. Ocean. Technol.*, 27, 1533–1546, doi:10.1175/2010JTECHO723.1, 2010.



- Lorthiois, T., Doxaran, D., Chami, M.: Daily and seasonal dynamics of suspended particles in the Rhone River plume based on remote sensing and field optical measurements, *Geo-Marine Lett.*, 32, 89–101, doi:10.1007/s00367-012-0274-2, 2012.
- Madsen, O.S.: Spectral wave-current bottom boundary layer flows. In Proceedings of the 24th international conference on coastal engineering, Kobe, Japan, 23–28 October 1994, American Society of Civil Engineers, USA, 384–398, 1994.
- 5 Middelburg, J.J., Soetaert, K., Herman, P.M.J., Heip, C.H.R.: Denitrification in marine sediments: A model study, *Global Biogeochem. Cycles*, 10, 661–673, 1996.
- Millot, C.: The Gulf of Lions' Hydrodynamics, *Cont. Shelf Res.*, 10, 885–894, 1990.
- Miralles, J., Arnaud, M., Radakovitch, O., Marion, C., Cagnat, X.: Radionuclide deposition in the Rhône River Prodelta (NW Mediterranean sea) in response to the December 2003 extreme flood, *Mar. Geol.*, 234, 179–189, doi:10.1016/j.margeo.2006.09.004, 2006.
- 10 Moll, A., Radach, G.: Review of three-dimensional ecological modelling related to the North Sea shelf system, *Prog. Oceanogr.*, 57, 175–217, doi:10.1016/S0079-6611(03)00067-3, 2003.
- Murrell, M.C., Lehrter, J.C.: Sediment and lower water column oxygen consumption in the seasonally hypoxic region of the Louisiana continental shelf, *Estuaries and Coasts*, 34, 912–924, doi:10.1007/s12237-010-9351-9, 2011.
- 15 Palanques, A., Durrieu de Madron, X., Puig, P., Fabres, J., Guillén, J., Calafat, A., Canals, M., Heussner, S., Bonnin, J.: Suspended sediment fluxes and transport processes in the Gulf of Lions submarine canyons: The role of storms and dense water cascading, *Mar. Geol.*, 234, 43–61, doi:10.1016/j.margeo.2006.09.002, 2006.
- Pastor, L., Cathalot, C., Deflandre, B., Viollier, E., Soetaert, K., Meysman, F.J.R., Ulses, C., Metzger, E., Rabouille, C.: 20 Modeling biogeochemical processes in sediments from the Rhône River prodelta area (NW Mediterranean Sea), *Biogeosciences*, 8, 1351–1366, doi:10.5194/bg-8-1351-2011, 2011a.
- Pastor, L., Deflandre, B., Viollier, E., Cathalot, C., Metzger, E., Rabouille, C., Escoubeyrou, K., Lloret, E., Pruski, A.M., Vétion, G., Desmalades, M., Buscaïl, R., Grémare, A.: Influence of the organic matter composition on benthic oxygen demand in the Rhône River prodelta (NW Mediterranean Sea), *Cont. Shelf Res.*, 31, 1008–1019, doi:10.1016/j.csr.2011.03.007, 2011b.
- 25 Pinazo, C., Marsaleix, P., Millet, B., Estournel, C., Véhil, R.: Spatial and temporal variability of phytoplankton biomass in upwelling areas of the northwestern mediterranean: a coupled physical and biogeochemical modelling approach, *J. Mar. Syst.*, 7, 161–191, doi:10.1016/0924-7963(95)00028-3, 1996.
- Pont, D.: Les débits solides du Rhône à proximité de son embouchure : données récentes (1994-1995) / The discharge of suspended sediments near to the mouth of the Rhône recent statistics (1994-1995), *Rev. géographie Lyon*, 72, 23–33, doi:10.3406/geoca.1997.4675, 1997.
- 30 Rabouille, C., Conley, D.J., Dai, M.H., Cai, W.-J., Chen, C.T. A., Lansard, B., Green, R., Yin, K., Harrison, P.J., Dagg, M., McKee, B.: Comparison of hypoxia among four river-dominated ocean margins: The Changjiang (Yangtze), Mississippi, Pearl, and Rhône rivers, *Cont. Shelf Res.*, 28, 1527–1537, doi:10.1016/j.csr.2008.01.020, 2008.



- Radakovitch, O., Charmasson, S., Arnaud, M., Bouisset, P.: 210-Pb and Caesium accumulation in the Rhone delta sediments, *Estuar. Coast. Shelf Sci.*, 48, 77–92, 1999.
- Rassmann, J., Lansard, B., Pozzato, L., Rabouille, C.: Carbonate chemistry in sediment pore waters of the Rhône River delta driven by early diagenesis (NW Mediterranean), *Biogeosciences Discuss.*, 1–35, doi:10.5194/bg-2016-212, 2016.
- 5 Roussiez, V., Ludwig, W., Monaco, A., Probst, J.-L., Bouloubassi, I., Buscail, R., Saragoni, G.: Sources and sinks of sediment-bound contaminants in the Gulf of Lions (NW Mediterranean Sea): A multi-tracer approach, *Cont. Shelf Res.*, 26, 1843–1857, doi:10.1016/j.csr.2006.04.010, 2006.
- Rowe, G.T., Chapman, P.: Continental shelf hypoxia: some nagging questions, *Gulf Mex. Sci.*, 2, 155–160, 2002.
- Shchepetkin, A.F.: A method for computing horizontal pressure-gradient force in an oceanic model with a nonaligned vertical coordinate, *J. Geophys. Res.*, 108, 3090, doi:10.1029/2001JC001047, 2003.
- 10 Shchepetkin, A.F., McWilliams, J.C.: Correction and commentary for “Ocean forecasting in terrain-following coordinates: Formulation and skill assessment of the regional ocean modeling system” by Haidvogel et al., *J. Comp. Phys.*, 227, pp. 3595–3624, *J. Comput. Phys.*, 228, 8985–9000, doi:10.1016/j.jcp.2009.09.002, 2009.
- Sherwood, C.R., Aretxabaleta, A., Harris, C.K., Rinehimer, J.P., Ferre, B., Verney, R.: Cohesive and mixed sediment model: Extension of the Community Sediment Transport Modeling System, 2016, in prep.
- 15 Sloth, N.P., Riemann, B., Nielsen, L.P., Blackburn, T.H.: Resilience of pelagic and benthic microbial communities to sediment resuspension in a coastal ecosystem, Knebel Vig, Denmark, *Estuar. Coast. Shelf Sci.*, 42, 405–415, doi:10.1006/ecss.1996.0027, 1996.
- Soetaert, K., Herman, P.M.J., Middelburg, J.J.: A model of early diagenetic processes from the shelf to abyssal depths, *Geochim. Cosmochim. Acta*, 60, 1019–1040, 1996a.
- 20 Soetaert, K., Herman, P.M.J., Middelburg, J.J.: Dynamic response of deep-sea sediments to seasonal variations: A model, *Limnol. Oceanogr.*, 41, 1651–1668, doi:10.4319/lo.1996.41.8.1651, 1996b.
- Soetaert, K., Herman, P.M.J., Middelburg, J.J., Heip, C.: Assessing organic matter mineralization, degradability and mixing rate in an ocean margin sediment (Northeast Atlantic) by diagenetic modeling, *J. Mar. Res.*, 56, 519–534, doi:10.1357/002224098321822401, 1998.
- 25 Soetaert, K., Middelburg, J.J., Herman, P.M.J., Buis, K.: On the coupling of benthic and pelagic biogeochemical models, *Earth Sci. Rev.*, 51, 173–201, doi:10.1016/S0012-8252(00)00004-0, 2000.
- Taylor, K.E.: Summarizing multiple aspects of model performance in a single diagram, *J. Geophys. Res.*, 106, 7183–7192, doi:10.1029/2000JD900719, 2001.
- 30 Tengberg, A., Almroth, E., Hall, P.: Resuspension and its effects on organic carbon recycling and nutrient exchange in coastal sediments: in situ measurements using new experimental technology, *J. Exp. Mar. Bio. Ecol.*, 285–286, 119–142, doi:10.1016/S0022-0981(02)00523-3, 2003.
- Tesi, T., Miserocchi, S., Goñi, M. a., Langone, L.: Source, transport and fate of terrestrial organic carbon on the western Mediterranean Sea, Gulf of Lions, France, *Mar. Chem.*, 105, 101–117, doi:10.1016/j.marchem.2007.01.005, 2007.



- Testa, J.M., Kemp, W.M.: Hypoxia-induced shifts in nitrogen and phosphorus cycling in Chesapeake Bay, *Limnol. Oceanogr.*, 57, 835–850, doi:10.4319/lo.2012.57.3.0835, 2012.
- Testa, J.M., Li, Y., Lee, Y.J., Li, M., Brady, D.C., Di Toro, D.M., Kemp, W.M., Fitzpatrick, J.J.: Quantifying the effects of nutrient loading on dissolved O₂ cycling and hypoxia in Chesapeake Bay using a coupled hydrodynamic-biochemical model, *J. Mar. Syst.*, 139, 139–158, doi:10.1016/j.jmarsys.2014.05.018, 2014.
- 5 Toussaint, F., Rabouille, C., Bombled, B., Abchiche, A., Aouji, O., Buchholtz, G., Clemençon, A., Geyskens, N., Repecaud, M., Pairaud, I., Verney, R., Tisnerat-Laborde, N.: A new device to follow temporal variations of oxygen demand in deltaic sediments: the LSCE benthic station, *Oceanogr. Methods*, 12, 729–741, doi:10.4319/lom.2014.12.729, 2014.
- Turner, R.E., Rabalais, N.N., Justic, D.: Gulf of Mexico hypoxia: alternate states and a legacy, *Environ. Sci. Technol.*, 42, 10 2323–7, 2008.
- Ulses, C., Estournel, C., Durrieu de Madron, X., Palanques, A.: Suspended sediment transport in the Gulf of Lions (NW Mediterranean): Impact of extreme storms and floods, *Cont. Shelf Res.*, 28, 2048–2070, doi:10.1016/j.csr.2008.01.015, 2008.
- van't Hoff, J.H.: Lectures on Theoretical and Physical Chemistry, Part I, Chemical Dynamics (translated by R. A. Lehfeldt), 15 Edward Arnold, London, 1898.
- Wainright, S.C., Hopkinson, C.S.: Effects of sediment resuspension on organic matter processing in coastal environments: A simulation model, *J. Mar. Syst.* 11, 353–368, 1997.
- Walsh, I., Fischer, K., Murray, D., Dymond, J.: Evidence for resuspension of rebound particles from near-bottom sediment traps, *Deep Sea Res. Part A, Oceanogr. Res. Pap.*, 35, 59–70. doi:10.1016/0198-0149(88)90057-X, 1988.
- 20 Wang, J., Wei, H., Lu, Y., Zhao, L.: Diffusive boundary layer influenced by bottom boundary hydrodynamics in tidal flows, *J. Geophys. Res. Ocean*, 118, 5994–6005, doi:10.1002/2013JC008900, 2013.
- Warner, J.C., Sherwood, C.R., Signell, R.P., Harris, C.K., Arango, H.G.: Development of a three-dimensional, regional, coupled wave, current, and sediment-transport model, *Comput. Geosci.*, 34, 1284–1306, doi:10.1016/j.cageo.2008.02.012, 2008.
- 25 Wiberg, P.L., Harris, C.K.: Desorption of p,p'-DDE from sediment during resuspension events on the Palos Verdes shelf, California: A modeling approach, *Cont. Shelf Res.*, 22, 1005–1023, 2002.
- Wijnsman, J.W.M., Herman, P.M.J., Middelburg, J.J., Soetaert, K.: A model for early diagenetic processes in sediments of the continental shelf of the Black Sea, *Estuar. Coast. Shelf Sci.*, 54, 403–421, doi:10.1006/ecss.2000.0655, 2002.
- Wilson, R.F., Fennel, K., Paul Mattern, J.: Simulating sediment–water exchange of nutrients and oxygen: A comparative 30 assessment of models against mesocosm observations, *Cont. Shelf Res.*, 63, 69–84, doi:10.1016/j.csr.2013.05.003, 2013.



Table 1: Description of symbols used in this paper.

Symbol	Description	Units
Agg_{lab}	Concentration of labile aggregates	$mmol\ N\ m^{-2}$
Agg_{ref}	Concentration of refractory aggregates	$mmol\ N\ m^{-2}$
$C_s\ tnew$	Concentration of dissolved tracer in the surficial seabed layer, for the new time step	$mmol\ m^{-2}$
$C_s\ told$	Concentration of dissolved tracer in the surficial seabed layer from the old time step	$mmol\ m^{-2}$
$C_w\ tnew$	Concentration of dissolved tracer in the bottom water column layer, for the new time step	$mmol\ m^{-2}$
$C_w\ told$	Concentration of dissolved tracer in the bottom water column layer from the old timestep	$mmol\ m^{-2}$
dO_2/dz_{OPD}	the slope of the vertical oxygen profile, averaged over the oxygen penetration depth, z_{OPD}	$mmol\ O_2\ m^{-4}$
D_i	Coefficient for diffusion within the seabed for seabed constituent i	$m^2\ s^{-1}$
D_{s-w}	Diffusion coefficient at the seabed water interface	$m^2\ s^{-1}$
dz	Grid cell thickness	m
E_{ised}	Mass of sediment from class $ised$	$kg\ m^{-2}$
f_{bur}	Fraction of organic matter that is buried in the seabed	---
f_{det}	Fraction of labile coagulated organic matter that is large detritus within the water column	---
f_{ised}	Fraction of the surficial seabed layer composed of sediment class $ised$	---
f_{lab}	Fraction of coagulated organic matter that is labile within the water column	---
$ised$	Index used for different sediment classes.	---
k_{O_2}	Half-saturation constant for O_2 limitation of aerobic remineralization	$mmol\ O_2\ m^{-2}$
$k_{O_2\ nit}$	Half-saturation constant for O_2 limitation of nitrification	$mmol\ O_2\ m^{-2}$
$k_{O_2\ oduox}$	Half-saturation constant for O_2 limitation of ODU oxidation	$mmol\ O_2\ m^{-2}$
k_{NO_3}	Half-saturation constant for NO_3 limitation of nitrate remineralization	$mmol\ N\ m^{-2}$
l_{O_2}	Half-saturation constant for O_2 inhibition of nitrate remineralization	$mmol\ O_2\ m^{-2}$
$l_{O_2\ anoxic}$	Half-saturation constant for O_2 inhibition of anoxic remineralization	$mmol\ O_2\ m^{-2}$
$l_{NO_3\ anoxic}$	Half-saturation constant for NO_3 inhibition of anoxic remineralization	$mmol\ N\ m^{-2}$
L_{BO}	Limitation of seabed oxygen consumption due to bottom boundary layer O_2 availability	---
L_{det}	Concentration of large detritus	$^1mmol\ N\ m^{-2}$
L_{tot}	Sum of the limitation factors on remineralization processes	---
M	Erosion rate parameter	$kg\ m^{-2}\ s^{-1}$
NO_3	Nitrate concentration	$^1mmol\ N\ m^{-2}$
$N_{high-res}$	Number of high-resolution seabed layers	---
$N_{med-res}$	Number of medium-resolution seabed layers	---
NH_4	Ammonium concentration	$^1mmol\ N\ m^{-2}$
$R_{anaerobic}$	Anaerobic Remineralization Rate in the seabed	$mmol\ C\ m^{-2}\ d^{-1}$
$R_{aerobic}$	Aerobic Remineralization Rate in the seabed	$mmol\ C\ m^{-2}\ d^{-1}$
R_{DNF}	Denitrification Rate in the seabed	$mmol\ C\ m^{-2}\ d^{-1}$
R_{nit}	Nitrification Rate in the seabed	$mmol\ N\ m^{-2}\ d^{-1}$
$R_{nit,max}$	Maximum Nitrification Rate in the seabed	d^{-1}
R_{oduox}	Oxidation Rate of ODUs in the seabed	$mmol\ O_2\ m^{-2}\ d^{-1}$
$R_{oduox,max}$	Maximum Oxidation Rate of ODUs in the seabed	d^{-1}
R_{POC}	Remineralization rate of particulate organic matter in the seabed	d^{-1}
$S_{inorganic}$	Inorganic sedimentation rate	$m\ y^{-1}$
$S_{organic}$	Particulate organic matter sedimentation rate	$gC\ m^{-2}\ y^{-1}$
O_2	Dissolved oxygen concentration	$^1mmol\ O_2\ m^{-2}$
$O_{2,OPD}$	Dissolved O_2 concentration at the oxygen penetration depth; equals zero by definition	$^1mmol\ O_2\ m^{-2}$
$O_{2,SWI}$	Dissolved oxygen concentration at the seabed-water interface	$mmol\ O_2\ m^{-2}$
ODU	Oxygen Demand Unit concentration	$^1mmol\ ODU\ m^{-2}$
POC	Particulate organic carbon concentration	$^1mmol\ C\ m^{-2}$
POM	Particulate organic matter concentration	$^1mmol\ N\ m^{-2}$
z_a	Thickness of seabed active transport layer	m
$z_{high-res}$	Thickness of high-resolution seabed layers	m
$z_{med-res}$	Thickness of medium-resolution seabed layers	m
z_{newdep}	Thickness of new deposition	m
z_{OPD}	Oxygen penetration depth into the seabed	m



z_{SWI}	Depth at the seabed water interface (SWI); equals zero in our coordinate system	m
z_{wl}	Thickness of bottom water column grid cell	m
Φ	Seabed porosity	---
τ_{bed}	Bed shear stress from waves and currents	Pa
τ_{crit}	Critical shear stress, assumed to be the same for all sediment classes.	Pa
$\tau_{crit,used}$	Critical shear stress for sediment class used.	Pa

[†]unless otherwise noted

Table 2: Description of phrases, acronyms, abbreviations, as used in this paper.

5	Acronym / Abbreviation	Description
	Active transport layer	Region of the seabed from which material can be entrained into the water column; synonymous with the phrase ‘active layer’ in sediment transport papers (Harris and Wiberg, 1997; Warner et al., 2008). In the model, the active transport layer is the same as the surficial seabed layer.
	Anoxic remineralization	Includes iron, manganese, and sulfur remineralization of organic matter, and methanogenesis, but not denitrification.
	Bottom boundary layer	The region of the water column within 4 m of the seabed where suspended sediment concentrations were high during resuspension events
	CSTMS	Community Sediment Transport Modeling System
	Diagenesis	Within this paper, ‘diagenesis’ is used to refer to models that account for organic matter remineralization and associated biogeochemical processes within the seabed. We note, however, that diagenesis is commonly used to refer to any physical, chemical, geological, or biological changes in sediment or sediment rock following deposition, prior to metamorphism.
	Diffusion at (or across) the seabed-water interface	Molecular diffusion of dissolved chemicals across the seabed-water interface. In the context of HydroBioSed, this refers to exchanges between the bottom water column grid cell and surficial seabed layer so that they are in equilibrium (see Appendix).
	Diffusion within the seabed	Molecular diffusion within the seabed; Referred to as ‘biodiffusion’ in other modeling papers when bioturbation is modeled as a diffusive process.
	HydroBioSed	The coupled hydrodynamic – sediment transport – water column and seabed biogeochemistry model developed and implemented in this study
	Local resuspension	Refers to resuspension in a one-dimensional (vertical) framework, neglecting horizontal transport processes.
	Module	Refers to a ‘sub-model’ within a model, e.g. the sediment transport module within ROMS
	Nitrate Remineralization	In this paper, synonymous with denitrification
	Nutrient(s)	Refers to refer to nitrogen and/or phosphorus. Does not include ODU _s
	ODU	Oxygen Demand Unit; one ODU is the number of moles of reduced chemical species that react with one mole of O ₂ when oxidized.
	Oxygen penetration depth (OPD)	Depth in the seabed at which oxygen decreased to zero.
	POM	Particulate organic matter
	Quiescent	Characterized by low-energy environmental conditions; i.e. used to refer non time periods with low waves and no resuspension in this paper
	Re-deposition	Deposition of particulates previously resuspended from the same location
	ROMS	Regional Ocean Modeling System
	Seabed	Region beneath the water column
	Sediment	Inorganic particles
	Steady state	Refers to models that do not change in time, e.g. due to wave-induced resuspension


Table 3: Environmental conditions and parameters for the Standard Model implementation.

Model Input/Parameter	Modeled Value	Literature Source
Hydrodynamic & Sediment Transport Parameters		
Water Depth	24 m	Pastor et al. (2011a)
Wave Height	Observed time-series	Toussaint et al. (2014)
Wave Period	10 s	Ulses et al. (2008), Palanques et al. (2006), Guillen et al. (2006)
Bottom Water Temperature	15 °C	Millot et al. (1990)
Surface Water Temperature	20 °C	Millot et al. (1990)
Bottom Water Salinity	35 psu	Panlanques et al., 2006; Cruzado and Velasquez, 1990
Surface Water Salinity	33 psu	Panlanques et al., 2006; Cruzado and Velasquez, 1990
Inorganic Sedimentation Rate	$S_{\text{inorganic}} = 10 \text{ cm y}^{-1}$ $= 14 \text{ kg m}^{-2} \text{ y}^{-1}$	Pastor et al. (2011a)
Fraction of Sediment that is Muddy Floes	80%	Roussiez et al. (2006), Ferre et al. (2005), Radkovitch et al. (1999)
Fraction of Sediment that is Sand	20%	Roussiez et al. (2006), Ferre et al. (2005), Radkovitch et al. (1999)
Settling Velocity of Muddy Floes	0.19 mm s^{-1}	Curran et al. (2007)
Settling Velocity of Sand	30 mm s^{-1}	Curran et al. (2007)
Critical Bed Shear Stress	$\tau_{\text{crit}} = 0.3 \text{ Pa}$	¹ Toussaint et al. (2014)
Erosion Rate Parameter	$M = 0.01 \text{ kg m}^{-2} \text{ s}^{-1}$	¹ Toussaint et al. (2014)
Porosity	$\Phi = 0.9$	Unpublished data
Sediment Density of Muddy floes	1048 kg m^{-3}	Curran et al. (2007)
Sediment Density of Sand	2650 kg m^{-3}	Curran et al. (2007)
Water Column Biogeochemical Parameters		
Oxygen Concentration	$253 \text{ mmol O}_2 \text{ m}^{-3}$	Toussaint et al. (2014), Pastor et al. (2011a)
Nitrate Concentration	$0.5 \text{ mmol N m}^{-3}$	Pastor et al. (2011a)
Ammonium Concentration	$5.8 \text{ mmol N m}^{-3}$	Pastor et al. (2011a)
ODU Concentration	$0 \text{ mmol O}_2 \text{ m}^{-3}$	Pastor et al. (2011a)
Phytoplankton Concentration	$0.03 \text{ mmol N m}^{-3}$	² Pastor et al. (2011a)
Zooplankton Concentration	$1.17 \text{ mmol N m}^{-3}$	² Pastor et al. (2011a)
Small Detritus Concentrations	$0.03 \text{ mmol N m}^{-3}$	² Pastor et al. (2011a)
Maximum Nitrification Rate	0.7 d^{-1}	Pinazo et al. (1996)
Coagulation Rate of Phytoplankton and Small Detritus	164.5 d^{-1}	² Pastor et al. (2011a)
Detritus & Aggregate Remineralization Rate	11 y^{-1}	Pinazo et al. (1996)
Settling (Sinking) Velocity of Phytoplankton	0.1 m d^{-1}	³ Fennel et al. (2006)
Settling (Sinking) Velocity of Large detritus	1.0 m d^{-1}	³ Fennel et al. (2006)
Settling (Sinking) Velocity of Small detritus	0.1 m d^{-1}	³ Fennel et al. (2006)
Settling (Sinking) Velocity of Labile Aggregates	16.416 m d^{-1}	Curran et al. (2007)
Settling (Sinking) Velocity of Refractory Aggregates	16.416 m d^{-1}	Curran et al. (2007)
Nudging parameter for Large detritus, Aggregates, Sediment	0 d^{-1}	---
Nudging parameter for NO ₃ , Phytoplankton, Small Detritus	0.02 d^{-1}	---
Nudging parameter for NH ₄ , Oxygen, ODU, Zooplankton	0.2 d^{-1}	---
POM Sedimentation rate	$S_{\text{organic}} = 657 \text{ gC m}^{-2} \text{ y}^{-1}$	Pastor et al. (2011a)
Partitioning of Refractory vs. Labile Organic Matter in Water Column	$f_{\text{lab}} = 0.5$	Pastor et al. (2011a)
Partitioning of Labile Aggregates vs. Large Detritus in	$f_{\text{det}} = 0.5$	Tesi et al. (2007) Pastor et al. (2011a)



Water Column	Seabed Biogeochemical Parameters	
Labile Organic Matter Remineralization Rate	11 y ⁻¹	Pastor et al. (2011a)
Refractory Organic Matter Remineralization Rate	0.31 y ⁻¹	Pastor et al. (2011a)
Ratio of mol C: mol N in Labile Organic Matter	7.10	Pastor et al. (2011a)
Ratio of mol C: mol N in Refractory Organic Matter	14.3	Pastor et al. (2011a)
Half Saturation Constant for O ₂ Limitation of Aerobic Remineralization	k _{O₂} = 1 μmol O ₂ L ⁻¹	Pastor et al. (2011a)
Half Saturation Constant for NO ₃ Limitation of Nitrate Remineralization (Denitrification)	k _{NO₃} = 100 μmol N L ⁻¹	Pastor et al. (2011a)
Half Saturation Constant for O ₂ Limitation of Nitrification	k _{O₂ nit} = 10 μmol O ₂ L ⁻¹	Pastor et al. (2011a)
Half Saturation Constant for O ₂ Limitation in ODU Oxidation	k _{O₂ oduox} = 2 μmol O ₂ L ⁻¹	Pastor et al. (2011a)
Half Saturation Constant for O ₂ Inhibition of Nitrate Remineralization (Denitrification)	I _{O₂} = 1 μmol O ₂ L ⁻¹	Pastor et al. (2011a)
Half Saturation Constant for O ₂ Inhibition of Anoxic Remineralization	I _{O₂ anoxic} = 1 μmol O ₂ L ⁻¹	Pastor et al. (2011a)
Half Saturation Constant for NO ₃ Inhibition of Anoxic Remineralization	I _{NO₃ anoxic} = 10 μmol NO ₃ L ⁻¹	Pastor et al. (2011a)
Maximum Nitrification Rate	R _{nit,max} = 100 d ⁻¹	Pastor et al. (2011a)
Maximum Oxidation Rate of Oxygen Demand Units	R _{oduox,max} = 20 d ⁻¹	Pastor et al. (2011a)
Fraction of ODUs Produced that are Solid and Inert	99.5%	Pastor et al. (2011a)
Diffusion Coefficient for Across Seabed-Water Interface	D _{s-w} = 1.08 × 10 ⁻⁹ m ² s ⁻¹	Toussaint et al. (2014)
Coefficients for Diffusion Within the Seabed	D _{particulates} = 2.55 × 10 ⁻¹⁰ m ² s ⁻¹ D _{O₂} = 11.99 × 10 ⁻¹⁰ m ² s ⁻¹ D _{NO₃} = 9.80 × 10 ⁻¹⁰ m ² s ⁻¹ D _{NH₄} = 10.04 × 10 ⁻¹⁰ m ² s ⁻¹ D _{ODU} = 4.01 × 10 ⁻¹⁰ m ² s ⁻¹	⁴ Pastor et al. (2011a)

¹Chosen based on time series of seabed elevation in Toussaint et al. (2014)

²Chosen based on organic sedimentation rate

³No local data

⁴These rates derive from the molecular diffusion rates, but were adjusted for the porosity and tortuosity of the seabed as described in Pastor et al., 2011a.

5

Table 4: List of sensitivity tests. Additionally, for each simulation listed here, an identical model run was completed that neglected resuspension (i.e. with $M = 0 \text{ kg/m}^2/\text{s}$; $\tau_{\text{crit}} = 10 \text{ Pa}$).

Sensitivity Test Abbreviation	Sensitivity Test Name	Changed Parameters and/or Parameterizations Relative to the Standard Model Run
R1	Low Erosion Rate Parameter	$M = 0.005 \text{ kg m}^{-2} \text{ s}^{-1}$
R2	High Erosion Rate Parameter	$M = 0.02 \text{ kg m}^{-2} \text{ s}^{-1}$
T1	Low Critical Shear Stress	$\tau_{\text{crit}} = 0.15 \text{ Pa}$
T2	High Critical Shear Stress	$\tau_{\text{crit}} = 0.6 \text{ Pa}$
S1	Low Inorganic Sedimentation	$S_{\text{inorganic}} = 0.05 \text{ m y}^{-1} = 7 \text{ kg m}^{-2} \text{ y}^{-1}$
S2	High Inorganic Sedimentation	$S_{\text{inorganic}} = 0.20 \text{ m y}^{-1} = 28 \text{ kg m}^{-2} \text{ y}^{-1}$
P1	Low Particulate Organic Sedimentation	$S_{\text{organic}} = 328.5 \text{ gC m}^{-2} \text{ y}^{-1}$
P2	High Particulate Organic Sedimentation	$S_{\text{organic}} = 1314 \text{ gC m}^{-2} \text{ y}^{-1}$
L1	Low Lability	$f_{\text{lab}} = 0.20$
L2	High Lability	$f_{\text{lab}} = 0.80$
B1	Low Seabed Diffusion	$D_i = \text{original values} * 0.5$
B2	High Seabed Diffusion	$D_i = \text{original values} * 2.0$
N1	Low Nitrification Rate	$R_{\text{nit,max}} = 50$
N2	High Nitrification Rate	$R_{\text{nit,max}} = 200$
O1	Low ODU Oxidation Rate	$R_{\text{oduox,max}} = 10$
O2	High ODU Oxidation Rate	$R_{\text{oduox,max}} = 40$



Table 5: Statistics for model-observation comparison, including the root mean square difference (RMSD) and the correlation coefficient (R). The mean and standard deviation of estimates from both the model and observations are also shown.

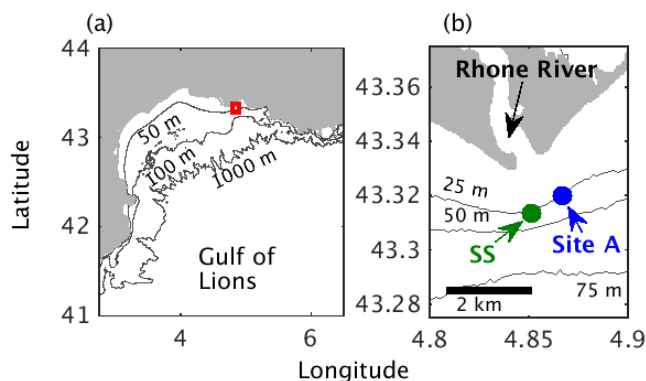
	RMSD	R	Mean ± Standard Deviation	
			Model	Observation
Seabed Height	1.39 cm	0.21	-0.52 ± 0.82 cm	-1.1 ± 1.2 cm
O ₂ Gradient	105 mol O ₂ m ⁻⁴	0.48	180 ± 118 mol O ₂ m ⁻⁴	173 ± 76 mol O ₂ m ⁻⁴

5

Table 6: O₂ Consumption (mmol O₂ m⁻² d⁻¹) in the seabed, bottom boundary layer, and combined seabed-BBL due to various processes over the two-month model run and during resuspension events. Abbreviations include: POM Rem. (particulate organic matter remineralization); ODU Ox (Oxidation of ODUs); Nit (nitrification); and “Seabed + BBL” (the combined seabed-bottom boundary layer region).

	Seabed				Bottom Boundary Layer				Seabed + BBL
	Total	POM Rem.	Nit.	ODU Ox.	Total	POM Rem.	Nit.	ODU Ox.	Total
2-Month Average	19	4.8	13	0.19	55	30.	14	0	73
Minimum Values	12	0.47	3.7	0.013	23	0.07	13	0	39
Maximum Values	35	18	32	0.63	190	160	20	0.003	217
Quiescent Conditions, i.e. value on June 1	18	4.6	13	0.19	23	0.73	13	0	41

10



15

Figure 1: a) Red box indicates location of panel (b) in the Gulf of Lions. b) Dots indicate our study site (SS; green) and Pastor et al. (2014)'s Site A (blue) offshore of the Rhone River. Bathymetric data (black lines) were obtained from the European Marine Observation and Data Network. Coastline data were obtained from the U.S. National Oceanic and Atmospheric Administration.

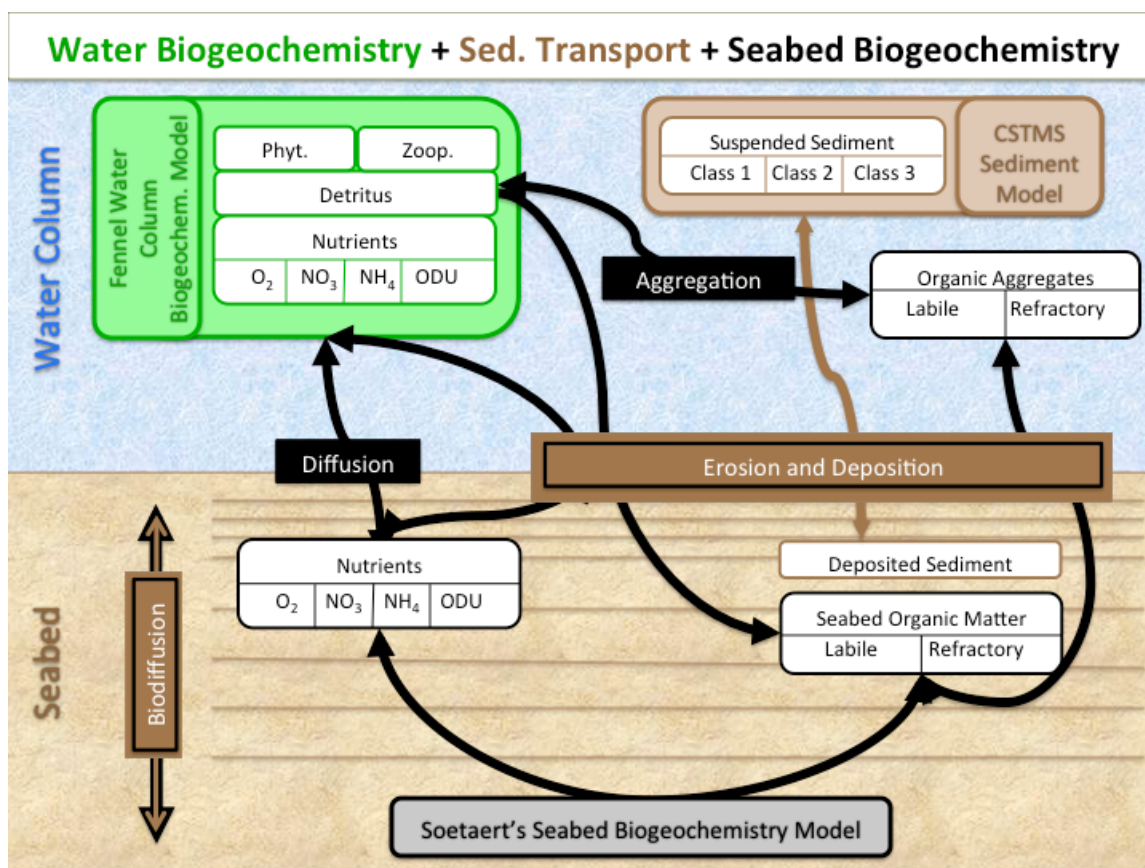


Figure 2: Schematic of links between the seabed biogeochemical module and other modules. The colors of the boxes and labels indicate processes associated with sediment transport (brown), water column biogeochemistry (green) and seabed biogeochemistry and model coupling (black). Abbreviations for this figure represent sediment (Sed.), biogeochemistry (Biogeochem.), phytoplankton (Phyt.) and zooplankton (Zoop.).

5

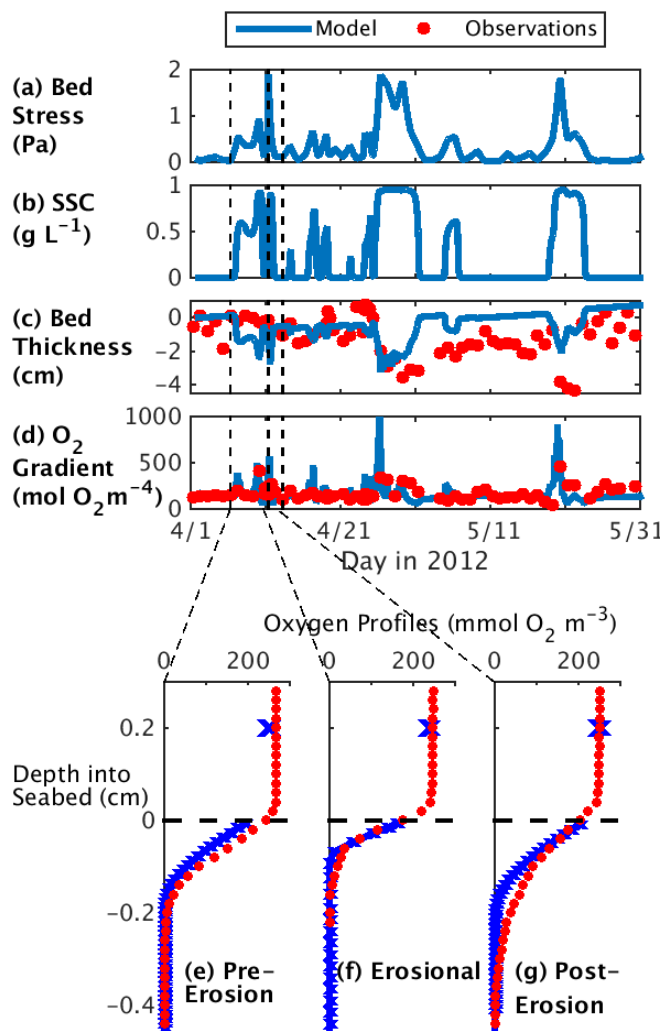


Figure 3: Time series of modeled (blue lines & x's) and observed (red dots; Toussaint et al., 2014) bed stress, near-bed suspended sediment concentrations, seabed height, and vertical oxygen gradient averaged over the oxic layer of the seabed (top 4 panels), and three examples of oxygen profiles before, during, and after an erosional event in early April (bottom panels). The dashed black lines in the bottom panels indicate the seabed-water interface.

5

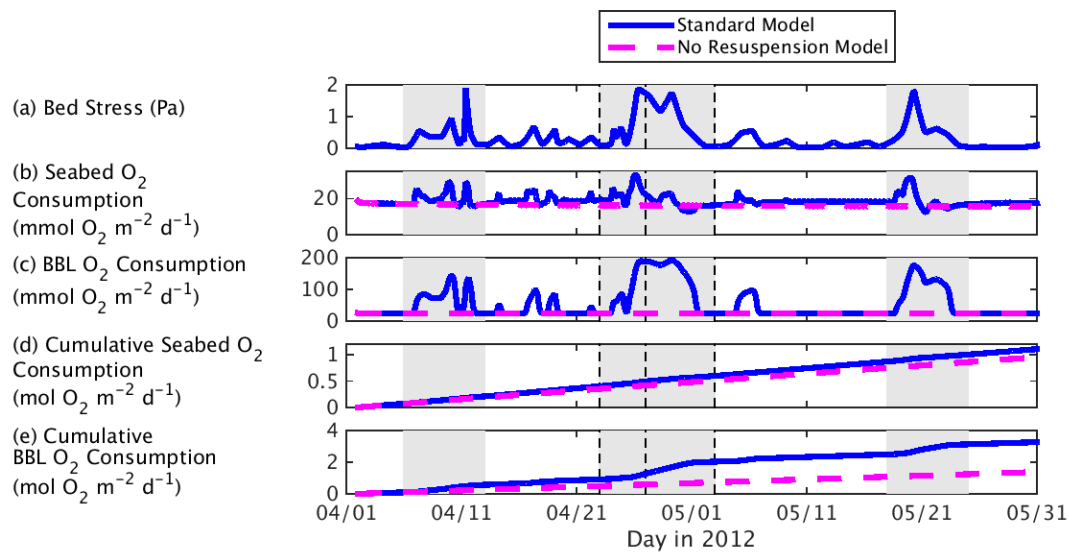
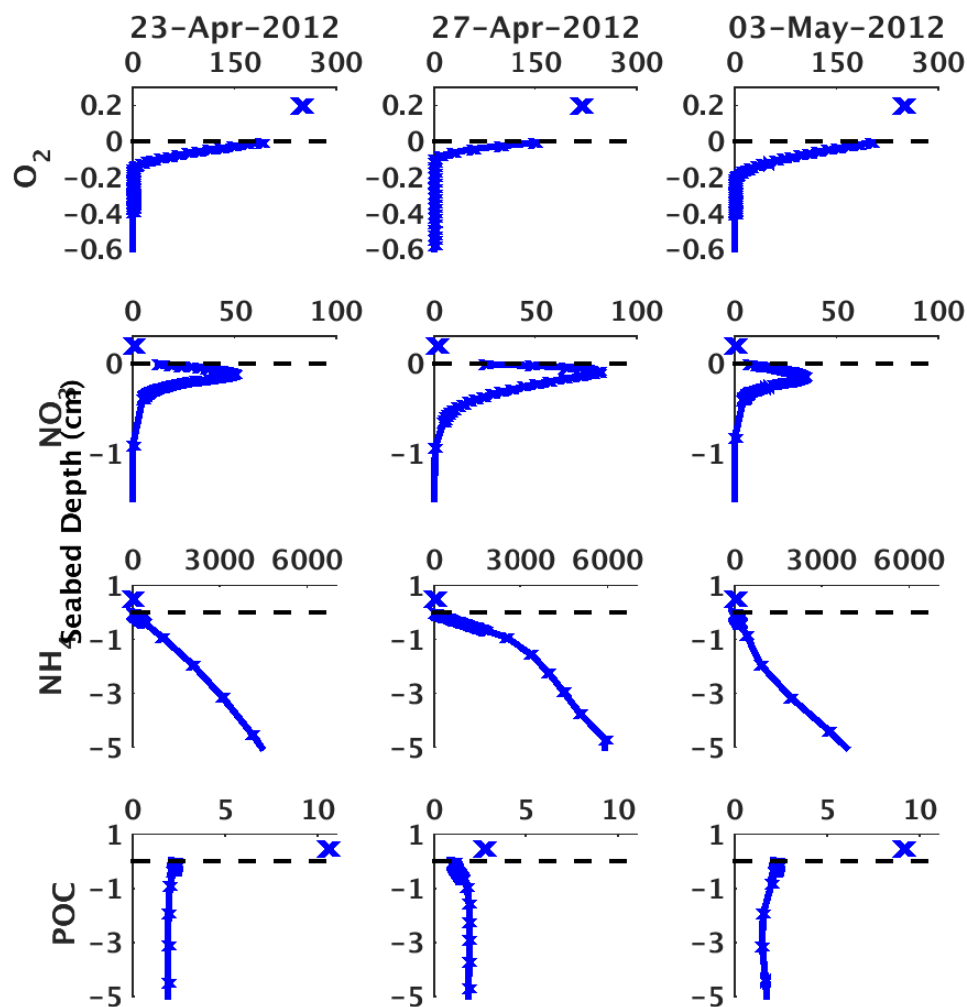


Figure 4: Time series of bed stress, and oxygen consumption in the seabed and bottom boundary layer for both the standard (blue solid line) and no-resuspension model runs (pink dashed line). Shading indicates resuspension time periods, including 6–11 April, 23 April–3 May, and 18–25 May 2012. The black dashed lines indicate the times at which profiles in Fig. 5 were estimated.



5 Figure 5: Seabed profiles of oxygen (top row; $\text{mmol O}_2 \text{ m}^{-3}$), nitrate (2nd row; mmol N m^{-3}), ammonium (3rd row; mmol N m^{-3}), and degradable particulate organic carbon (POC; bottom row; dry weight (%)) from the standard model run for times immediately preceding the late April resuspension event (left column), during the erosional period (center column), and during the depositional period (right column). See Fig. 4 for the times at which the profiles were estimated. The black dashed lines indicate the seabed water interface, and all seabed depths are given relative to this interface. The 'X's indicate near-bed values for the water column.

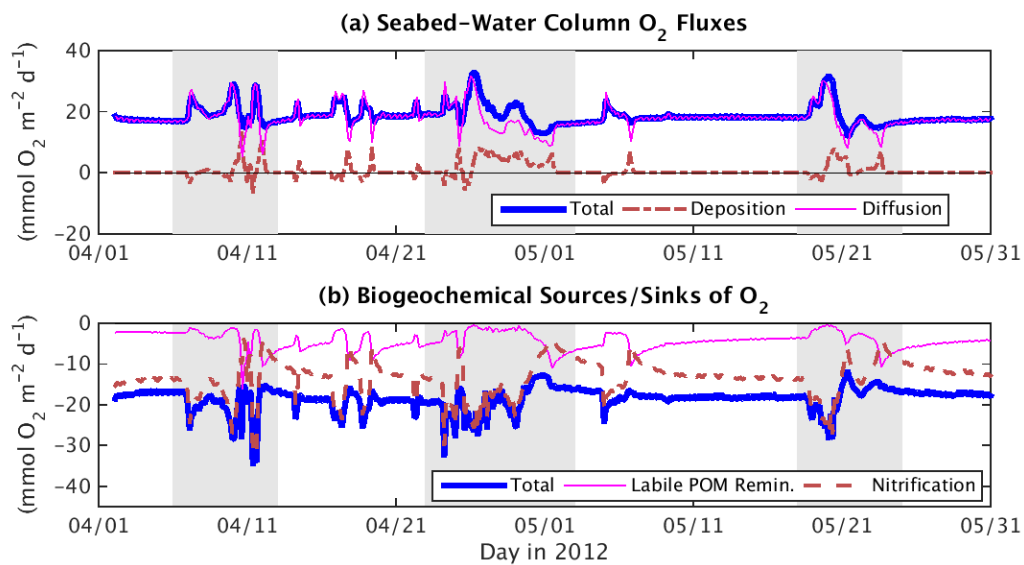


Figure 6: Physical (top) and biogeochemical (bottom) fluxes of oxygen within the seabed for the standard model run. Sources and sinks of oxygen to the seabed are positive and negative, respectively. Small biogeochemical sinks $<1 \text{ mmol O}_2 \text{ m}^{-2} \text{ d}^{-1}$ (ODU oxidation and remineralization of refractory POM) are not shown. Shading indicates resuspension time periods, including April 6–11, April 23–May 3, and May 18–25, 2012.

5

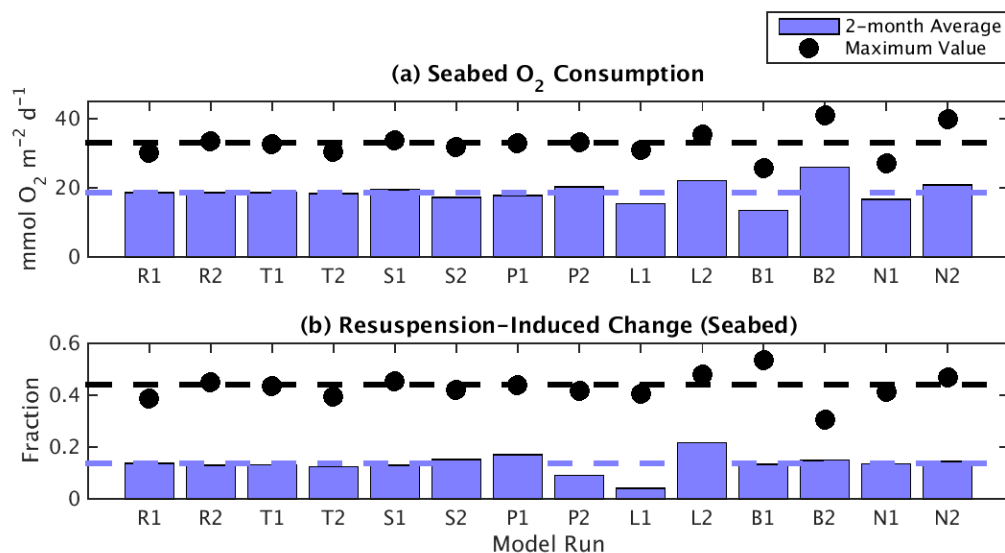


Figure 7: (a) Rate of oxygen consumption in the seabed for each sensitivity test listed in Table 4. (b) Fraction of oxygen consumption induced by resuspension, calculated by dividing the difference between each sensitivity test and its no-resuspension model run by the value from the sensitivity test. In both panels, bars represent averages over two months. Dots indicate the maximum values during this two-month period (which occurred during resuspension events). The dashed lines represent values from the standard model run, with the color of the line consistent with the type of data it represents (i.e. two-month average or maximum value).

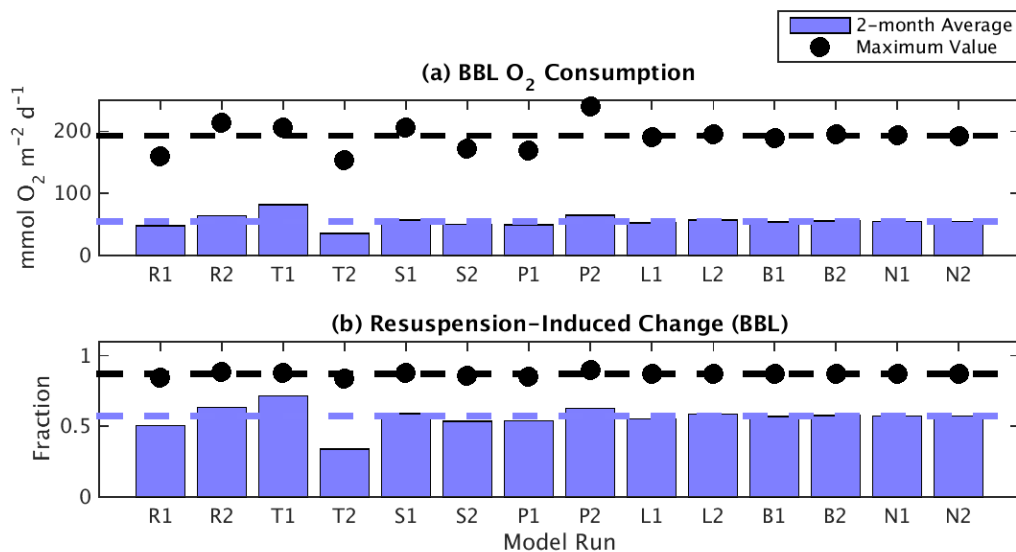


Figure 8: Same as Fig. 7, but for oxygen consumption in the bottom boundary layer (i.e. the bottom 4 m of the water column).

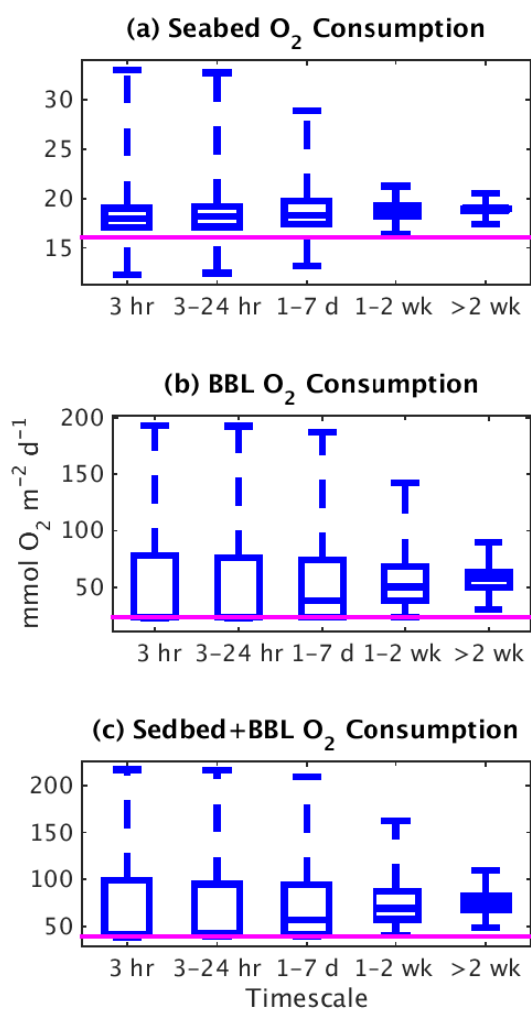


Figure 9: Box and whisker plots indicating the 0th, 25th, 50th, 75th, and 100th percentiles of (a) seabed, (b) bottom boundary layer and (c) combined seabed-bottom boundary layer oxygen consumption averaged over different timescales for the standard model run. The pink lines indicate estimates from the no-resuspension model run.